ARCME manuscript No.
(will be inserted by the editor)

Analysis of an unconditionally convergent stabilized finite element formulation for incompressible magnetohydrodynamics

Santiago Badia · Ramon Codina · Ramon Planas

Received: date / Accepted: date

Abstract In this work, we analyze a recently proposed stabilized finite element formulation for the approximation of the resistive magnetohydrodynamics equations. The novelty of this formulation with respect to existing ones is the fact that it always converges to the physical solution, even when it is singular. We have performed a detailed stability and convergence analysis of the formulation in a simplified setting. From the convergence analysis, we infer that a particular type of meshes with a macro-element structure is needed, which can be easily obtained after a straight modification of any original mesh.

Keywords magnetohydrodynamics · finite elements · singular solutions · stabilized finite element methods

The work of the first and third authors was funded by the European Research Council under the FP7 Programme Ideas through the Starting Grant No. 258443 - COMFUS: Computational Methods for Fusion Technology and the project FUSSIM, Ref. ENE2011-28556, from the Spanish Government. The second author has been partially supported by the Consolider-Ingenio project TECNOFUS, Ref. CSD2008-00079, from the Spanish Ministry of Science and Innovation, and from the ICREA Acadèmia Program, from the Catalan Government. Finally, the third author would like to acknowledge the support received from the *Universitat Politècnica de Catalunya (UPC)* and from the *Col.legi d'Enginyers de Camins, Canals i Ports de Catalunya*.

S. Badia
Centre Internacional de Metodes Numerics en Enginyeria (CIMNE) and Universitat Politècnica de Catalunya (UPC),
Parc Mediterrani de la Tecnologia, UPC, Esteve Terradas 5, 08860 Castelldefels, Spain
E-mail: sbadia@cimne.upc.edu

R. Codina
Universitat Politècnica de Catalunya (UPC),
Campus Nord, Jordi Girona 1-3, Edifici C1, 08034 Barcelona, Spain.

R. Planas
Centre Internacional de Metodes Numerics en Enginyeria (CIMNE) and Universitat Politècnica de Catalunya (UPC),
Parc Mediterrani de la Tecnologia, Esteve Terradas 5, 08860 Castelldefels, Spain

1 Introduction

In this work, we analyze a numerical formulation for the approximation of the incompressible visco-resistive magnetohydrodynamics (MHD) system, which models incompressible viscous and electrically conducting fluids under electromagnetic fields (see [27]). Many conforming numerical approximations to this problem have been proposed so far. There are different equivalent formulations of the continuous magnetic sub-problem, namely saddle-point and (weighted) exact penalty formulations (see [42] and [34,2,35,24,25], respectively). The first one leads to a double-saddle-point formulation for the MHD system. A Galerkin finite element (FE) approximation of the resulting problem has been proposed and analyzed by Schötzau in [42]. It is well-known that saddle-point formulations require to choose particular mixed FE spaces satisfying discrete versions of the so-called inf-sup conditions (see e.g. [18]). Instead, a weighted exact penalty formulation has been used in [34]. This formulation allows to simplify implementation issues but introduces a new complication, the definition of the weight function (see [25]). Alternative formulations have been proposed for a regularized version of the system, based on an exact penalty formulation [33]. These methods must be used with caution, since they converge to spurious solutions when the exact magnetic field is not smooth. Non-conforming approximations of discontinuous Galerkin type have been designed in [38]. They have good numerical properties, but the increase in CPU cost –degrees of freedom– of these formulations (with respect to conforming formulations) is severe for realistic large-scale applications. For the Maxwell equations alone, alternative approximations based on nodal Lagrangian FEs can be found e.g. in [16,15,28]. We refer to [39,3] for the application of residual-free bubbles to MHD and [9] for a two-level stabilization method with Scott-Vogelius FEs.

Since the resistive MHD system loses coercivity as the Reynolds and magnetic Reynolds numbers increase, i.e. convection-type terms become dominant, the previous formulations are unstable unless the mesh size is sufficientely refined, which is impractical. In order to treat this problem, as well as the previous ones, some stabilized FE formulations have been proposed for resistive MHD in [10,11,30,31,21,22,43]. These formulations are appealing in terms of implementation issues, since arbitrary order Lagrangian FE spaces can be used for all the unknowns and include convection-type stabilization. However, these formulations are based on the regularized functional setting of the problem, and so, restricted to smooth or convex domains (see [25]). They are accurate for regular magnetic solutions but tend to spurious (unphysical) solutions otherwise. A further improvement is the formulation in [7,8], which always converges to the exact (physical) solution, even when it is singular. In this work, we carry out a numerical analysis of this formulation in order to prove stability and unconditional convergence in the correct norms while keeping optimal *a priori* error estimates for smooth solutions.

The outline of this work is the following. First, the MHD problem of interest is stated in Section 2. The stabilized FE formulation is introduced in Section 3. We present a detailed stability and convergence analysis for the stationary and linearized problem in Sections 4 and 5 respectively. The behavior of the method in advection-dominated regimes is addressed in Section 6. The possible extension of these results

to nonlinear problem is analyzed in Section 7. Section 8 is devoted to the numerical experiments. We finish the work by drawing some conclusions in Section 9.

2 Problem statement

2.1 The strong form

The incompressible visco-resistive MHD system of partial differential equations consists of the Navier-Stokes equations coupled to the (simplified) Maxwell equations via the Lorentz force. A linearized version of this system of equations reads as follows: find a velocity field $\mathbf{u}(\mathbf{x})$, a (kinematic) pressure $p(\mathbf{x})$, an induced magnetic (induction) field $\mathbf{b}(\mathbf{x})$ and a magnetic pseudo-pressure $r(\mathbf{x})$ such that

$$\mathbf{a}\cdot\nabla\mathbf{u} - \nu\Delta\mathbf{u} + \nabla p - (\nabla\times\mathbf{b})\times\mathbf{d} = \mathbf{f}_{\mathrm{u}}, \tag{2.1a}$$

$$\nabla\cdot\mathbf{u} = g_{\mathrm{u}}, \tag{2.1b}$$

$$\lambda\nabla\times(\nabla\times\mathbf{b}) + \nabla r - \nabla\times(\mathbf{u}\times\mathbf{d}) = \mathbf{f}_{\mathrm{b}}, \tag{2.1c}$$

$$\nabla\cdot\mathbf{b} = g_{\mathrm{b}}, \tag{2.1d}$$

in $\mathbf{x}\in\Omega$, where $\Omega\subset\mathbb{R}^d$ is the spatial open bounded domain filled by the fluid (assumed polyhedral in the finite element approximation), d being the space dimension. With regard to the physical parameters that describe the fluid, ρ is its density, μ_{f} the fluid viscosity, μ_{m} the magnetic permeability and σ the electric conductivity. Further, $\nu := \mu_{\mathrm{f}}\rho^{-1}$ and $\lambda := (\rho\mu_{\mathrm{m}}^2\sigma)^{-1}$. In this work, we consider all physical properties constant; we refer to [5] for discontinuous physical coefficients for the electromagnetic problem. $(\mathbf{a},\mathbf{d})$ is the point around which the system has been linearized. In order to recover the nonlinear case, $(\mathbf{a},\mathbf{d})$ must be replaced by $(\mathbf{u},\kappa\mathbf{b})$, where $\kappa := (\rho\mu_{\mathrm{m}})^{-1}$. Regularity conditions for $(\mathbf{a},\mathbf{d})$ are discussed later. $\mathbf{f}_{\mathrm{u}}$ and $\mathbf{f}_{\mathrm{b}}$ are the forcing terms, $\mathbf{f}_{\mathrm{b}}$ being solenoidal.

We can also consider the non-dimensionalized equations, by introducing the characteristic quantities (U_0, B_0, L_0) for the velocity, magnetic field and length of the domain. In this case, the equations are characterized by three adimensional parameters, the hydrodynamic Reynolds number Re, the coupling number N and the magnetic Reynolds number Rm. If (2.1a)-(2.1d) are written in dimensionless form, we should identify $\mathrm{Re} = \nu^{-1}$, $\mathrm{N} = \kappa$ and $\mathrm{Rm} = \kappa\lambda^{-1}$. The coupling number is usually written in terms of the Hartmann number Ha as $\mathrm{N} = \mathrm{Ha}^2(\mathrm{Re}\,\mathrm{Rm})^{-1}$.

Let us remark the fact that we have introduced g_{b} and g_{u}. We are only interested in the case when both functions are zero, but this generalization will allow us to reuse the following stability results in the convergence analysis. These equations must be supplemented with appropriate boundary conditions.

In order to introduce the boundary conditions, let us consider two disjoint partitions of the domain boundary $\Gamma\equiv\partial\Omega$:

$$\Gamma = \Gamma_{\mathrm{f,e}}\cup\Gamma_{\mathrm{f,n}}, \qquad \Gamma = \Gamma_{\mathrm{m,e}}\cup\Gamma_{\mathrm{m,n}},$$

where the first subscript denotes the subproblem (f for fluid and m for magnetic) and the second one the type of boundary condition (e for essential and n for natural).

Then, the fluid sub-problem is supplemented with the standard boundary conditions:

$$\mathbf{u} = \mathbf{u}_\Gamma \quad \text{on } \Gamma_{\text{f,e}}, \qquad -p\mathbf{n} + \nu \mathbf{n} \cdot \nabla \mathbf{u} = \boldsymbol{\sigma}_{n,\Gamma} \quad \text{on } \Gamma_{\text{f,n}},$$

where $\mathbf{u}_\Gamma(\mathbf{x})$ and $\boldsymbol{\sigma}_{n,\Gamma}(\mathbf{x})$ are the trace and normal stress prescribed; $\mathbf{n}(\mathbf{x})$ denotes the normal vector on Γ pointing outwards from Ω. With regard to the magnetic sub-problem, we consider the set of ideal boundary conditions:

$$\mathbf{n} \times \mathbf{b} = \mathbf{n} \times \mathbf{b}_\Gamma, \quad r = 0 \quad \text{on } \Gamma_{\text{m,e}}, \qquad \mathbf{n} \cdot \mathbf{b} = \mathbf{n} \cdot \mathbf{b}_\Gamma, \quad \mathbf{n} \times (\nabla \times \mathbf{b}) = \mathbf{J}_\Gamma \quad \text{on } \Gamma_{\text{m,n}},$$

where $\mathbf{n} \cdot \mathbf{b}_\Gamma$ and $\mathbf{n} \times \mathbf{b}_\Gamma$ are the normal and tangential traces to be prescribed; clearly, $\mathbf{J}_\Gamma \cdot \mathbf{n}$ must vanish.

Taking the divergence of (2.1c), we easily infer that $r = 0$. Unfortunately, this is not true in general for the discretized system. For numerical purposes, it is more suitable to explicitly enforce (2.1d) via a Lagrange multiplier, the magnetic pseudo-pressure $r(\mathbf{x})$.

2.2 The weak form

Let us introduce some notation to set up the weak form of the problem. As usual, Sobolev spaces of functions whose derivatives of order up to m belong to $L^2(\Omega)$ are denoted by $H^m(\Omega)$; $H^1_0(\Omega)$ is the subspace of $H^1(\Omega)$ of functions vanishing on $\partial\Omega$. The space of vector functions with components in $L^2(\Omega)$ and with divergence also in $L^2(\Omega)$ is denoted $H(\text{div};\Omega)$; if the components are $L^2(\Omega)$ and the curl is in $L^2(\Omega)^d$ the space is denoted $H(\mathbf{curl};\Omega)$. $H(\text{div}\,0;\Omega)$ is the subspace of $L^2(\Omega)^d$ of divergence free vector functions.

The inner product of $f, g \in L^2(\Omega)$ is represented as (f,g), whereas $\langle f,g \rangle$ is used to denote the integral $\int_\Omega fg$ whenever it makes sense; this in particular applies for the duality between $H^1_0(\Omega)$ and its topological dual $H^{-1}(\Omega)$. The same notation is used for both scalar and vector valued functions. Given a normed functional space X, its norm is written as $\|\cdot\|_X$, with the abbreviations $\|\cdot\|_{L^2(\Omega)} \equiv \|\cdot\|$, $\|\cdot\|_{H^m(\Omega)} \equiv \|\cdot\|_m$, $\|\cdot\|_{H^{-1}(\Omega)} \equiv \|\cdot\|_{-1}$, $\|\cdot\|_{H(\mathbf{curl};\Omega)} \equiv \|\cdot\|_{\mathbf{curl}}$. Finally, the symbol $\lesssim$ is used to denote $\leq$ up to positive constants that do not depend on numerical or physical parameters.

Let us consider the functional setting in which the system of equations (2.1) is well-posed. For the sake of clarity, we will consider homogeneous essential boundary conditions; in any case, the extension to the most general case is standard. We introduce the vectorial functional spaces:

$$V = \{\mathbf{v} \in H^1(\Omega)^d \text{ such that } \mathbf{v} = \mathbf{0} \text{ on } \Gamma\},$$
$$C = \{\mathbf{c} \in H(\mathbf{curl};\Omega) \text{ such that } \mathbf{n} \times \mathbf{c} = \mathbf{0} \text{ on } \Gamma\},$$

for the velocity and magnetic field functions, respectively. Further, the space for fluid pressures is $Q \equiv L^2_0(\Omega)$ and the one for magnetic pseudo-pressures $S \equiv H^1_0(\Omega)$. Now, we can state the stationary MHD problem at hand in its weak form as follows: find

$\mathbf{u} \in V$, $\mathbf{b} \in C$, $p \in Q$ and $r \in S$ such that

$$\langle \mathbf{a} \cdot \nabla \mathbf{u}, \mathbf{v} \rangle + (\nu \nabla \mathbf{u}, \nabla \mathbf{v}) - (p, \nabla \cdot \mathbf{v}) - \langle (\nabla \times \mathbf{b}) \times \mathbf{d}, \mathbf{v} \rangle = \langle \mathbf{f}_{\mathrm{u}}, \mathbf{v} \rangle, \tag{2.2a}$$

$$(q, \nabla \cdot \mathbf{u}) = \langle g_{\mathrm{u}}, q \rangle, \tag{2.2b}$$

$$(\lambda \nabla \times \mathbf{b}, \nabla \times \mathbf{c}) - \langle \nabla \times (\mathbf{u} \times \mathbf{d}), \mathbf{c} \rangle + (\nabla r, \mathbf{c}) = \langle \mathbf{f}_{\mathrm{b}}, \mathbf{c} \rangle, \tag{2.2c}$$

$$-(\nabla s, \mathbf{b}) = \langle g_{\mathrm{b}}, s \rangle, \tag{2.2d}$$

for any $(\mathbf{v}, \mathbf{c}, q, s) \in V \times C \times Q \times S$. Let us show that $r \equiv 0$ in (2.2). Taking $\mathbf{c} = \nabla r$ (which clearly belongs to C) in (2.2c), and using the fact that $\nabla \times \nabla r = \mathbf{0}$ and $\nabla \cdot \mathbf{f}_{\mathrm{b}} = 0$ a.e. in Ω, we obtain $\|\nabla r\| = 0$. Since r vanishes on $\partial\Omega$, it implies $r \equiv 0$ a.e. in Ω by virtue of Poincaré's inequality. We refer to [35, Propositions 3.4 and 3.5] for the completion of the proof.

Let us re-write system (2.2) in compact manner as:

$$\mathscr{A}((\mathbf{u}, \mathbf{b}, p, r), (\mathbf{v}, \mathbf{c}, q, s)) = \mathscr{F}(\mathbf{v}, \mathbf{c}, q, s), \quad \forall (\mathbf{v}, \mathbf{c}, q, s) \in V \times C \times Q \times S.$$

with the obvious definition of the bilinear form $\mathscr{A}$ and the linear form $\mathscr{F}$.

In the following, we consider infima and suprema with respect to functions in some space different from the zero function. For the sake of brevity, we will omit the fact that the zero function cannot be picked. Problem (2.2) is well-posed due to the inf-sup conditions

$$\inf_{q \in Q} \sup_{\mathbf{v} \in V} \frac{(q, \nabla \cdot \mathbf{v})}{\|q\| \|\mathbf{v}\|_1} \geq \beta_{\mathrm{f}} > 0, \qquad \inf_{s \in S} \sup_{\mathbf{c} \in C} \frac{(\nabla s, \mathbf{c})}{\|s\|_1 \|\mathbf{c}\|_{H(\mathbf{curl};\Omega)}} \geq \beta_{\mathrm{m}} > 0, \tag{2.3}$$

that are known to be true at the continuous level, as well as the Poincaré-Friedrichs inequalities

$$\begin{aligned} \|\mathbf{v}\|_1 &\leq C_{\mathrm{P},1} \|\nabla \mathbf{v}\| && \text{for } \mathbf{v} \in H_0^1(\Omega)^d, \\ \|\mathbf{c}\|_{H(\mathbf{curl};\Omega)} &\leq C_{\mathrm{P},2} \|\nabla \times \mathbf{c}\| && \text{for } \mathbf{c} \in C \cap H(\operatorname{div} 0; \Omega), \end{aligned} \tag{2.4}$$

e.g., see [40, Corollary 3.51].

From the standard theory of saddle-point problems, well-posedness of the MHD system (2.2) is proved in the next theorem.

Theorem 2.1 *The following inf-sup condition is satisfied,*

$$\inf_{(\mathbf{u},\mathbf{b},p,r) \in V \times C \times Q \times S} \sup_{(\mathbf{v},\mathbf{c},q,s) \in V \times C \times Q \times S} \frac{\mathscr{A}((\mathbf{u}, \mathbf{b}, p, r), (\mathbf{v}, \mathbf{c}, q, s))}{\|(\mathbf{u}, \mathbf{b}, p, r)\|_{\mathrm{Gal}} \times \|(\mathbf{v}, \mathbf{c}, q, s)\|_{\mathrm{Gal}}} \geq \beta > 0. \tag{2.5}$$

As a consequence, formulation (2.2) is well-posed.

Proof: We can easily check that $\mathscr{A}((\mathbf{u}, \mathbf{b}, 0, 0), (\mathbf{v}, \mathbf{c}, 0, 0))$ is a bilinear, continuous and coercive form when it is restricted to $V \cap H(\operatorname{div} 0; \Omega) \times C \cap H(\operatorname{div} 0; \Omega)$. It is a direct consequence of the Poincaré-Friedrichs inequalities (2.4). This result, together with the inf-sup conditions (2.3) are necessary and sufficient conditions for proving (2.5) (see [29, Proposition 2.36]). We know from the theory of saddle-point problems that (2.2) is well-posed if and only if condition (2.5) is satisfied (see [29, Theorem 2.34]). □

3 A stabilized FE formulation suitable for singular magnetic solutions

Let us present now the spatial discretization we propose. Let $\{\mathscr{T}_h\}$, with $0 < h \leq 1$, be a family of partitions of the domain Ω, such that $h\text{diam}(\Omega) \leq \max\{\text{diam}(K) : K \in \mathscr{T}_h\}$. For simplicity we assume Ω polyhedral and $\{\mathscr{T}_h\}$ quasi-uniform. Summation over all the element domains K is denoted as $\sum_K$. Finite element spaces and FE functions are identified with the subscript h. Only conforming approximations are considered, i.e., the FE spaces where the unknowns are sought are $V_h \subset V$, $C_h \subset C$, $Q_h \subset Q$ and $S_h \subset S$. In particular, we will use $\mathscr{C}^0$ Lagrangian finite element interpolations of an arbitrary order for all the unknowns. Given two functions f and g piecewise polynomial on each $K \in \mathscr{T}_h$, we define $(f,g)_h := \sum_K \int_K f\, g$ and $\|f\|_h := (f,f)_h^{1/2}$.

Since we assume $\{\mathscr{T}_h\}$ quasi-uniform, the following inverse inequality holds:

$$\|\nabla v_h\|_{L^2(K)} \leq \frac{C_{\text{inv}}}{h}\|v_h\|_{L^2(K)}, \qquad K \in \mathscr{T}_h, \tag{3.1}$$

for a positive constant C_{inv} and for all piecewise polynomial functions v_h.

We consider a residual-based stabilized FE formulation for the MHD problem. This type of formulation does not change the statement of the continuous problem but modifies the way the discretization is performed. Instead of considering only those terms that come from a Galerkin discretization, this type of formulation includes additional terms, that are always proportional to some residual, and so, consistent. In order for this approach to be effective, the new terms must provide stability over the Lagrange multiplier-type unknowns which allows one to circumvent discrete inf-sup conditions, as well as convection stability (see e.g. [20]). In order to obtain a numerical algorithm suitable for singular solutions and avoiding the need to define weighting functions that require information about the placement of singularities, we stick to the double saddle-point formulation (2.2). The resulting method has been stated in Algorithm 1; we refer to [7] for a motivation of the method.

We consider the following norms that will be used hereafter:

$$\|(\mathbf{v},\mathbf{c},q,s)\|_{\text{Gal}} = \nu^{\frac{1}{2}}\|\mathbf{v}\|_1 + \lambda^{\frac{1}{2}}\|\mathbf{c}\|_{\mathbf{curl}} + \frac{1}{\nu^{\frac{1}{2}}}\|q\| + \frac{L_0}{\lambda^{\frac{1}{2}}}\|s\|_1, \tag{3.3a}$$

$$\begin{aligned}|(\mathbf{v},\mathbf{c},q,s)|_{\text{stab}} = {} & \|\tau_1^{\frac{1}{2}} X_{\text{u}}(\mathbf{v},q,\mathbf{c})\|_h + \|\tau_2^{\frac{1}{2}}\nabla\cdot\mathbf{v}\| + \|\tau_3^{\frac{1}{2}}\nabla\times(\mathbf{v}\times\mathbf{d})\| \\ & + \|\tau_4^{\frac{1}{2}}\nabla s\| + \|\tau_5^{\frac{1}{2}}\nabla\cdot\mathbf{c}\|,\end{aligned} \tag{3.3b}$$

$$\|(\mathbf{v},\mathbf{c},q,s)\|_{\text{stab,w}} = \nu^{\frac{1}{2}}\|\mathbf{v}\|_1 + \lambda^{\frac{1}{2}}\|\nabla\times\mathbf{c}\| + |(\mathbf{v},\mathbf{c},q,s)|_{\text{stab}}, \tag{3.3c}$$

$$\|(\mathbf{v},\mathbf{c},q,s)\|_{\text{stab,s}} = \frac{\lambda^{\frac{1}{2}}}{L_0}\|\mathbf{c}\| + \frac{1}{\nu^{\frac{1}{2}}}\|q\| + \|(\mathbf{v},\mathbf{c},q,s)\|_{\text{stab,w}}, \tag{3.3d}$$

where L_0 is a length scale of the problem (see [4] for a discussion about its meaning and possible ways to choose it).

Norm (3.3a) is the continuous norm in which the problem is well-posed, and the Galerkin norm when using stable mixed FEs. The extra stability due to the form $\mathscr{S}$ is given by the semi-norm (3.3b). Norm (3.3c) is the one that adds the stability that comes from the coercive terms in $\mathscr{A}$ to the one that comes from $\mathscr{S}$. Finally, norm

Algorithm 1: Stabilized FE formulation

Find $(\mathbf{u}_h, \mathbf{b}_h, p_h, r_h) \in V_h \times C_h \times Q_h \times S_h$ such that

$$\mathscr{A}_{\text{stab}}((\mathbf{u}_h, \mathbf{b}_h, p_h, r_h), (\mathbf{v}_h, \mathbf{c}_h, q_h, s_h)) = \mathscr{F}_{\text{stab}}(\mathbf{v}_h, \mathbf{c}_h, q_h, s_h), \tag{3.2}$$

for any $(\mathbf{v}_h, \mathbf{c}_h, q_h, s_h) \in V_h \times C_h \times Q_h \times S_h$, where

$$\begin{aligned}\mathscr{A}_{\text{stab}}((\mathbf{u}_h, \mathbf{b}_h, p_h, r_h), (\mathbf{v}_h, \mathbf{c}_h, q_h, s_h)) =& \mathscr{A}((\mathbf{u}_h, \mathbf{b}_h, p_h, r_h), (\mathbf{v}_h, \mathbf{c}_h, q_h, s_h)) \\ &+ \mathscr{S}((\mathbf{u}_h, \mathbf{b}_h, p_h, r_h), (\mathbf{v}_h, \mathbf{c}_h, q_h, s_h)),\end{aligned}$$

with the stabilization terms

$$\begin{aligned}\mathscr{S}((\mathbf{u}_h, \mathbf{b}_h, p_h, r_h), (\mathbf{v}_h, \mathbf{c}_h, q_h, s_h)) =& (\tau_1 (X_{\text{u}}(\mathbf{u}_h, p_h, \mathbf{b}_h) - \nu \Delta \mathbf{u}_h), X_{\text{u}}(\mathbf{v}_h, q_h, \mathbf{c}_h) + \nu \Delta \mathbf{v}_h)_h \\ &+ (\tau_2 \nabla \cdot \mathbf{u}_h, \nabla \cdot \mathbf{v}_h) \\ &+ (\tau_3 (\nabla \times (\mathbf{u}_h \times \mathbf{d}) - \lambda \nabla \times (\nabla \times \mathbf{b}_h)), \nabla \times (\mathbf{v}_h \times \mathbf{d}) + \lambda \nabla \times (\nabla \times \mathbf{c}_h))_h \\ &+ (\tau_4 \nabla r_h, \nabla s_h) + (\tau_5 \nabla \cdot \mathbf{b}_h, \nabla \cdot \mathbf{c}_h),\end{aligned}$$

and

$$\begin{aligned}\mathscr{F}_{\text{stab}}(\mathbf{v}_h, \mathbf{c}_h, q_h, s_h) =& \mathscr{F}(\mathbf{v}_h, \mathbf{c}_h, q_h, s_h) + (\tau_1 \mathbf{f}_{\text{u}}, X_{\text{u}}(\mathbf{v}_h, q_h, \mathbf{c}_h) + \nu \Delta \mathbf{v}_h)_h + (\tau_2 g_{\text{u}}, \nabla \cdot \mathbf{v}_h) \\ &- (\tau_3 \mathbf{f}_{\text{b}}, \nabla \times (\mathbf{v}_h \times \mathbf{d}) + \lambda \nabla \times (\nabla \times \mathbf{c}_h))_h + (\tau_5 g_{\text{b}}, \nabla \cdot \mathbf{c}_h).\end{aligned}$$

We use the notation $X_{\text{u}}(\mathbf{v}_h, q_h, \mathbf{c}_h) := \mathbf{a} \cdot \nabla \mathbf{v}_h + \nabla q_h - (\nabla \times \mathbf{c}_h) \times \mathbf{d}$. The stabilization parameters have the following expressions within each element K:

$$\begin{aligned}&\tau_1 := (\alpha)^{-1} \left(1 + \tfrac{\phi}{\sqrt{\alpha \gamma}}\right)^{-1}, \ \tau_2 := c_5 \tfrac{h^2}{\tau_1}, \quad \tau_3 := \gamma^{-1} \left(1 + \tfrac{\phi}{\sqrt{\alpha \gamma}}\right)^{-1}, \\ &\tau_4 := c_6 \tfrac{L_0^2}{\lambda}, \qquad\qquad \tau_5 := c_7 \tfrac{h^2 \lambda}{L_0^2},\end{aligned}$$

with

$$\alpha := c_1 \frac{\|\mathbf{a}\|_{L^\infty(\Omega)}}{h} + c_2 \frac{\nu}{h^2}, \qquad \phi := c_3 \frac{\|\mathbf{d}\|_{L^\infty(\Omega)}}{h}, \qquad \gamma := c_4 \frac{\lambda}{h^2}.$$

$c_1, \ldots, c_5$ are algorithmic constants that must satisfy $c_1 > \frac{2}{C_{\text{inv}}^2}$ and $c_3 > \frac{2}{C_{\text{inv}}^2}$ and L_0 is a length scale of the problem.

(3.3d) is the sum of the weak stability norm $\|\cdot\|_{\text{stab,w}}$ terms and the additional terms that are present in $\|\cdot\|_{\text{Gal}}$. Obviously, $\|(\mathbf{v}, \mathbf{c}, q, s)\|_{\text{Gal}} \leq \|(\mathbf{v}, \mathbf{c}, q, s)\|_{\text{stab,s}}$.

4 Stability analysis

In this section, we analyze the stability properties of the stabilized FE formulation in Algorithm 1. First, we prove coercivity of the stabilized form $\mathscr{A}_{\text{stab}}$ in the weak stabilized norm. Next, we prove a weak inf-sup which includes $\|\mathbf{b}\|$ and $\|p\|$ control. We attain this result relying on the continuous inf-sup condition (2.5) proved in Theorem 2.1. We absorb the length scale coefficients in the constants, since it clarifies the exposition.

Lemma 4.1 *Forms $\mathscr{A}_{\text{stab}}$ and $\mathscr{A}$ satisfy the following properties:*

(i) Weak coercivity of $\mathscr{A}_{\text{stab}}$: Assuming that $\mathbf{a} \in H^1(\Omega)^d$ and $\mathbf{d} \in H(\mathbf{curl};\Omega)$, it holds

$$\frac{1}{2}\|(\mathbf{u}_h,\mathbf{b}_h,p_h,r_h)\|^2_{\text{stab,w}} \leq \mathscr{A}_{\text{stab}}((\mathbf{u}_h,\mathbf{b}_h,p_h,r_h),(\mathbf{u}_h,\mathbf{b}_h,p_h,r_h)),$$

for any $(\mathbf{u}_h,\mathbf{b}_h,p_h,r_h) \in V_h \times C_h \times Q_h \times S_h$.

(ii) Weak inf-sup condition for $\mathscr{A}$: Assuming that $\mathbf{a} \in H^1(\Omega)^d$ and $\mathbf{d} \in L^{d+\varepsilon}(\Omega)^d$, it holds

$$\begin{aligned}\|(\mathbf{u}_h,\mathbf{b}_h,p_h,r_h)\|_{\text{Gal}} - \sigma\|(\mathbf{u}_h,\mathbf{b}_h,p_h,r_h)\|_{\text{stab,w}} \\ \lesssim \sup_{(\mathbf{v}_h,s_h)\in V_h\times S_h} \frac{\mathscr{A}((\mathbf{u}_h,\mathbf{b}_h,p_h,r_h),(\mathbf{v}_h,\mathbf{0},0,s_h))}{\|(\mathbf{v}_h,\mathbf{0},0,s_h)\|_{\text{Gal}}}\end{aligned}$$

for any $(\mathbf{u}_h,\mathbf{b}_h,p_h,r_h) \in V_h \times C_h \times Q_h \times S_h$, where

$$\sigma = c_\sigma\left(1 + \frac{h}{\nu^{\frac{1}{2}}\tau_1^{\frac{1}{2}}} + \frac{\|\mathbf{d}\|_{L^{d+\varepsilon}(\Omega)}}{\sqrt{\nu\lambda}}\right)$$

for $\varepsilon \in (0,3)$ arbitrary small and c_σ a positive constant independent of physical and numerical parameters.

Proof: Let us prove the first result. Using the equality $(a+b)(a-b) = a^2 - b^2$, it is straightforward to check that

$$\begin{aligned}\mathscr{A}_{\text{stab}}((\mathbf{u}_h,\mathbf{b}_h,p_h,r_h),(\mathbf{u}_h,\mathbf{b}_h,p_h,r_h)) = \nu\|\nabla\mathbf{u}_h\|^2 + \lambda\|\nabla\times\mathbf{b}_h\|^2 + |(\mathbf{u}_h,\mathbf{b}_h,p_h,r_h)|^2_{\text{stab}} \\ - \|\tau_1^{\frac{1}{2}}\nu\Delta\mathbf{u}_h\|^2_h - \|\tau_3^{\frac{1}{2}}\lambda\nabla\times(\nabla\times\mathbf{b}_h)\|^2_h.\end{aligned}$$

We have used the relation $\int_\Omega((\nabla\times\mathbf{b})\times\mathbf{d})\cdot\mathbf{u} = -\int_\Omega \nabla\times(\mathbf{u}\times\mathbf{d})\cdot\mathbf{b}$ that holds for any $\mathbf{b},\mathbf{d} \in H(\mathbf{curl};\Omega)$ and $\mathbf{u} \in H^1(\Omega)^3$. The last two terms can be bounded for FE functions, by using the inverse inequality (3.1) elementwise:

$$\|\tau_1^{\frac{1}{2}}\nu\Delta\mathbf{u}_h\|^2_h + \|\tau_3^{\frac{1}{2}}\lambda\nabla\times(\nabla\times\mathbf{b}_h)\|^2_h \leq \frac{1}{2}(\nu\|\nabla\mathbf{u}_h\|^2 + \lambda\|\nabla\times\mathbf{b}_h\|^2),$$

since $\frac{\tau_1\nu}{h^2} \leq \frac{1}{2}$ and $\frac{\tau_3\lambda}{h^2} \leq \frac{1}{2}$ from the definition of the stabilization parameters. Full control over $\mathbf{u}_h$ in $H^1(\Omega)^3$ is consequence of Poincaré's inequality. It proves the weak coercivity.

In order to prove the weak inf-sup condition, let us invoke the continuous inf-sup condition (2.5) for the full MHD system, which can be stated as follows: for any $(\mathbf{u}_h,\mathbf{b}_h,p_h,r_h) \in V_h \times C_h \times Q_h \times S_h$ there exists $(\mathbf{v},\mathbf{c},q,s) \in V \times C \times Q \times S$ with unit Galerkin norm such that

$$\|(\mathbf{u}_h,\mathbf{b}_h,p_h,r_h)\|_{\text{Gal}} \leq \mathscr{A}((\mathbf{u}_h,\mathbf{b}_h,p_h,r_h),(\mathbf{v},\mathbf{c},q,s)).$$

Now, we have that

$$\begin{aligned}\mathscr{A}((\mathbf{u}_h,\mathbf{b}_h,p_h,r_h),(\mathbf{v},\mathbf{c},q,s)) =& \mathscr{A}((\mathbf{u}_h,\mathbf{b}_h,p_h,r_h),(\varepsilon_h(\mathbf{v}),\mathbf{c},q,\varepsilon_h(s))) \\ &+ \mathscr{A}((\mathbf{u}_h,\mathbf{b}_h,p_h,r_h),(\pi_h(\mathbf{v}),\mathbf{0},0,\pi_h(s))),\end{aligned} \quad (4.1)$$

where $\varepsilon_h(v) := v - \pi_h(v)$ and $\pi_h(v)$ is a continuous FE interpolant in $H^1(\Omega)$ of a function v (scalar or vector valued) with optimal interpolation properties that preserves null traces, e.g. the Scott-Zhang interpolant [17].

Let us define the following functions:

$$q(\delta,d) = \begin{cases} \frac{2}{1-2\delta}, & \text{for} d = 2 \\ \frac{12-2\delta}{4-\delta}, & \text{for} d = 3 \end{cases}, \qquad q(\delta,d)' = \begin{cases} \frac{1}{\delta}, & \text{for} d = 2 \\ 6-\delta, & \text{for} d = 3 \end{cases}.$$

where $\delta \in (0, \frac{1}{2})$. We note that $\frac{1}{q(\delta,d)} + \frac{1}{q(\delta,d)'} = \frac{1}{2}$. Now, we can prove the continuity result

$$(\nabla \times (\mathbf{u} \times \mathbf{d}), \mathbf{c}) \lesssim \|\mathbf{u}\|_{L^{q(\delta,d)'}(\Omega)} \|\mathbf{d}\|_{L^{q(\delta,d)}(\Omega)} \|\nabla \times \mathbf{c}\| \lesssim \|\mathbf{u}\|_1 \|\mathbf{d}\|_{L^{q(\delta,d)}(\Omega)} \|\nabla \times \mathbf{c}\|,$$

which holds for any $\delta \in (0, \frac{1}{2})$.We have used the compact imbedding $H^1(\Omega) \hookrightarrow L^q(\Omega)$ that holds for $q \in [1,\infty)$ in dimension two and for $q \in [1,6)$ in dimension three. Noting that $q(\delta,d)'$ belongs to these intervals in both dimensions, we prove the result. Now, we bound the first term in the RHS of (4.1) as follows:

$$\begin{aligned}
&\mathscr{A}((\mathbf{u}_h, \mathbf{b}_h, p_h, r_h), (\varepsilon_h(\mathbf{v}), \mathbf{c}, q, \varepsilon_h(s))) \\
&\quad \lesssim \|X_{\mathrm{u}}(\mathbf{u}_h, p_h, \mathbf{b}_h)\| \|\varepsilon_h(\mathbf{v})\| + \|\nabla \cdot \mathbf{b}_h\| \|\varepsilon_h(s)\| + \nu \|\nabla \mathbf{u}_h\| \|\nabla \varepsilon_h(\mathbf{v})\| \\
&\qquad + \|\nabla \cdot \mathbf{u}_h\| \|q\| + \lambda \|\nabla \times \mathbf{b}_h\| \|\nabla \times \mathbf{c}\| + \|\nabla r_h\| \|\mathbf{c}\| + \|\mathbf{u}_h\|_1 \|\mathbf{d}\|_{L^{q(\delta,d)}(\Omega)} \|\nabla \times \mathbf{c}\| \\
&\quad \lesssim \frac{h}{\nu^{\frac{1}{2}}} \|X_{\mathrm{u}}(\mathbf{u}_h, p_h, \mathbf{b}_h)\| + h\lambda^{\frac{1}{2}} \|\nabla \cdot \mathbf{b}_h\| + (1 + \frac{\|\mathbf{d}\|_{L^{q(\delta,d)}(\Omega)}}{\sqrt{\nu\lambda}}) \nu^{\frac{1}{2}} \|\mathbf{u}_h\|_1 \\
&\qquad + \lambda^{\frac{1}{2}} \|\nabla \times \mathbf{b}_h\| + \frac{1}{\lambda^{\frac{1}{2}}} \|\nabla r_h\| \\
&\quad \lesssim \left(1 + \frac{h}{\nu^{\frac{1}{2}} \tau_1^{\frac{1}{2}}} + \frac{\|\mathbf{d}\|_{L^{q(\delta,d)}(\Omega)}}{\sqrt{\nu\lambda}}\right) \|(\mathbf{u}_h, p_h, \mathbf{b}_h, r_h)\|_{\mathrm{stab,w}},
\end{aligned}$$

where we have used the interpolation error estimate $\|\varepsilon_h(v)\| \lesssim h\|v\|_1$, integration-by-parts, Schwarz's inequality and the previous continuity result. The second term in the right-hand side of (4.1) is easily handled by using the $H^1(\Omega)$ stability of the projector $\pi_h(\cdot)$. Noting that for any $\varepsilon \in (0,3)$ there exists $\delta > 0$ such that $d + \varepsilon > q(\delta,d)$, we prove the result. Let us stress the fact that ε can be taken arbitrarily small. □

Combining the previous lemmas, we readily get a weak inf-sup condition which provides control in the strong stabilized form.

Corollary 4.1 *Under the assumption that* $\mathbf{a} \in H^1(\Omega)^d$ *and* $\mathbf{d} \in L^{d+\varepsilon}(\Omega)^d$ *for an arbitrarily small* $\varepsilon > 0$*, the following inequality holds for any* $(\mathbf{u}_h, \mathbf{b}_h, p_h, r_h) \in V_h \times C_h \times Q_h \times S_h$*,*

$$\begin{aligned}
\|(\mathbf{u}_h, \mathbf{b}_h, p_h, r_h)\|_{\mathrm{stab,s}} \lesssim &\sup_{(\mathbf{v}_h, s_h) \in V_h \times S_h} \frac{\mathscr{A}((\mathbf{u}_h, \mathbf{b}_h, p_h, r_h), (\mathbf{v}_h, \mathbf{0}, 0, s_h))}{\|(\mathbf{v}_h, \mathbf{0}, 0, s_h)\|_{\mathrm{Gal}}} \\
&+ \sigma \mathscr{A}_{\mathrm{stab}}((\mathbf{u}_h, \mathbf{b}_h, p_h, r_h), (\mathbf{u}_h, \mathbf{b}_h, p_h, r_h))^{\frac{1}{2}}. \qquad (4.2)
\end{aligned}$$

Now, we are in position to provide bounds of the FE solution of the MHD problem in Algorithm 1 with respect to the data.

Theorem 4.1 *The solution* $(\mathbf{u}_h, \mathbf{b}_h, p_h, r_h)$ *of the FE problem (3.2) satisfies:*

(i) Weak stability: For $\mathbf{a} \in H^1(\Omega)^d$ *and* $\mathbf{d} \in H(\mathbf{curl}; \Omega)$*, it holds*

$$\|(\mathbf{u}_h, \mathbf{b}_h, p_h, r_h)\|_{\text{stab,w}} \leq \sup_{(\mathbf{v}_h, \mathbf{c}_h, q_h, s_h) \in V_h \times C_h \times Q_h \times S_h} \frac{\mathscr{F}_{\text{stab}}(\mathbf{v}_h, \mathbf{c}_h, q_h, s_h)}{\|\mathbf{v}_h, \mathbf{c}_h, q_h, s_h\|_{\text{stab,w}}} \tag{4.3}$$

(ii) Strong stability: For $\mathbf{a} \in L^\infty(\Omega)^d$ *and* $\mathbf{d} \in W^{1,d+\varepsilon}(\Omega)^d \cap L^\infty(\Omega)^d$ *for an arbitrarily small* $\varepsilon > 0$*, it holds*

$$\begin{aligned} \|(\mathbf{u}_h, \mathbf{b}_h, p_h, r_h)\|_{\text{stab,s}} \leq & \xi \|(\mathbf{u}_h, \mathbf{b}_h, p_h, r_h)\|_{\text{stab,w}} \\ & + \sup_{(\mathbf{v}_h, s_h) \in V_h \times S_h} \frac{|\mathscr{F}_{\text{stab}}(\mathbf{v}_h, \mathbf{0}, 0, s_h)|}{\|(\mathbf{v}_h, \mathbf{0}, 0, s_h)\|_{\text{stab,s}}}, \end{aligned} \tag{4.4}$$

with the constant

$$\begin{aligned} \xi = & 1 + \frac{\tau_1^{\frac{1}{2}}}{\nu^{\frac{1}{2}}} \|\mathbf{a}\|_{L^\infty(\Omega)} + \frac{\tau_3^{\frac{1}{2}}}{\nu^{\frac{1}{2}}} (\|\nabla \mathbf{d}\|_{L^{d+\varepsilon}(\Omega)} + \|\mathbf{d}\|_{L^\infty(\Omega)}) + \frac{\|\mathbf{d}\|_{L^{d+\varepsilon}(\Omega)}}{\sqrt{\nu \lambda}} \\ & + \left(1 + \frac{\|\mathbf{a}\|_{L^\infty(\Omega)} h}{\nu}\right)^{\frac{1}{2}} \left(1 + \frac{\|\mathbf{d}\|_{L^\infty(\Omega)} h}{\sqrt{\lambda \nu} \sqrt{1 + \frac{\|\mathbf{a}\|_{L^\infty(\Omega)} h}{\nu}}}\right)^{\frac{1}{2}}. \end{aligned}$$

Proof: We readily prove the weak stability invoking Lemma 4.1 and the stabilized FE system (3.2). Strong stability is proved using Corollary 4.1. The second term in the right-hand side of (4.2) is readily handled by the weak stability (4.3). On the other hand, the first term is bounded as follows:

$$\begin{aligned} & \mathscr{A}((\mathbf{u}_h, \mathbf{b}_h, p_h, r_h), (\pi_h(\mathbf{v}), \mathbf{0}, 0, \pi_h(s))) = \\ & - (\tau_1 (X_{\text{u}}(\mathbf{u}_h, p_h, \mathbf{b}_h) - \nu \Delta \mathbf{u}_h), \mathbf{a} \cdot \nabla \pi_h(\mathbf{v}) + \nu \Delta \pi_h(\mathbf{v}))_h \\ & - (\tau_2 \nabla \cdot \mathbf{u}_h, \nabla \cdot \pi_h(\mathbf{v})) - (\tau_3 (\nabla \times (\mathbf{u}_h \times \mathbf{d}) - \lambda \nabla \times (\nabla \times \mathbf{b}_h)), \nabla \times (\pi_h(\mathbf{v}) \times \mathbf{d}))_h \\ & - (\tau_4 \nabla r_h, \nabla \pi_h(s)) + \mathscr{F}_{\text{stab}}(\pi_h(\mathbf{v}), \mathbf{0}, 0, \pi_h(s)) \\ & \leq \left(\|(\mathbf{u}_h, \mathbf{b}_h, p_h, r_h)\|_{\text{stab,w}} + \sup_{(\mathbf{v}_h, s_h) \in V_h \times S_h} \frac{|\mathscr{F}_{\text{stab}}(\mathbf{v}_h, \mathbf{0}, 0, s_h)|}{\|(\mathbf{v}_h, \mathbf{0}, 0, s_h)\|_{\text{stab,s}}} \right) \\ & \quad \times (\tau_1^{\frac{1}{2}} \|\mathbf{a} \cdot \nabla \pi_h(\mathbf{v})\| + \tau_1^{\frac{1}{2}} \|\nu \Delta \pi_h(\mathbf{v})\|_h + \tau_2^{\frac{1}{2}} \|\nabla \cdot \pi_h(\mathbf{v})\| + \tau_3^{\frac{1}{2}} \|\nabla \times (\pi_h(\mathbf{v}) \times \mathbf{d})\| \\ & \quad + \tau_4^{\frac{1}{2}} \|\nabla \pi_h(s)\| + \nu^{\frac{1}{2}} \|\pi_h(\mathbf{v})\|_1 \|). \end{aligned} \tag{4.5}$$

Let us work on the right-hand side of the previous inequality. Using the stability properties of the projector $\pi_h(\cdot)$, we obtain:

$$\tau_1^{\frac{1}{2}} \|\mathbf{a} \cdot \nabla \pi_h(\mathbf{v})\| \leq \tau_1^{\frac{1}{2}} \|\mathbf{a}\|_{L^\infty(\Omega)} \|\nabla \mathbf{v}\|.$$

The same arguments allow us to get the following bound:

$$\begin{aligned}\tau_3^{\frac{1}{2}}\|\nabla\times(\pi_h(\mathbf{v})\times\mathbf{d})\| &\lesssim \tau_3^{\frac{1}{2}}(\|\mathbf{v}\|_{L^{q(\delta,d)'}(\Omega)}\|\nabla\mathbf{d}\|_{L^{q(\delta,d)}(\Omega)}+\|\nabla\mathbf{v}\|\|\mathbf{d}\|_{L^\infty(\Omega)})\\ &\lesssim \tau_3^{\frac{1}{2}}\|\mathbf{v}\|_1(\|\nabla\mathbf{d}\|_{L^{q(\delta,d)}(\Omega)}+\|\mathbf{d}\|_{L^\infty(\Omega)}),\end{aligned}$$

where we have used the vector analysis formula

$$\nabla\times(\mathbf{a}\times\mathbf{b})=\mathbf{b}\cdot\nabla\mathbf{a}-\mathbf{b}(\nabla\cdot\mathbf{a})-\mathbf{a}\cdot\nabla\mathbf{b}+\mathbf{a}(\nabla\cdot\mathbf{b}),$$

that holds for any smooth vector fields $\mathbf{a}$ and $\mathbf{b}$, and similar arguments as those above. Invoking these bounds in (4.5), we easily get:

$$\begin{aligned}\mathscr{A}((\mathbf{u}_h,\mathbf{b}_h,p_h,r_h),(\pi_h(\mathbf{v}),\mathbf{0},0,\pi_h(s)))\lesssim{}&\|(\mathbf{v}_h,\mathbf{0},0,s_h)\|_{\mathrm{Gal}}\times\|(\mathbf{u}_h,\mathbf{b}_h,p_h,r_h)\|_{\mathrm{stab,w}}\\ &\times\left(\frac{\tau_1^{\frac{1}{2}}}{\nu^{\frac{1}{2}}}\|\mathbf{a}\|_{L^\infty(\Omega)}+\frac{\tau_3^{\frac{1}{2}}}{\nu^{\frac{1}{2}}}(\|\nabla\mathbf{d}\|_{L^{q(\delta,d)}(\Omega)}+\|\mathbf{d}\|_{L^\infty(\Omega)})\right).\end{aligned}$$

Now, let us rewrite some coefficients by using the definition of the stabilization parameters:

$$\frac{h}{\nu^{\frac{1}{2}}\tau_1^{\frac{1}{2}}}=\left(1+\frac{\|\mathbf{a}\|_{L^\infty(\Omega)}h}{\nu}\right)^{\frac{1}{2}}\left(1+\frac{\|\mathbf{d}\|_{L^\infty(\Omega)}h}{\sqrt{\nu\lambda}\sqrt{1+\frac{\|\mathbf{a}\|_{L^\infty(\Omega)}h}{\nu}}}\right)^{\frac{1}{2}}.$$

Using again that for small enough $\varepsilon>0$ there exists $\delta>0$ such that $d+\varepsilon>q(\delta,d)$, we prove the theorem. □

Remark 4.1 In practice, both $\mathbf{a}$ and $\mathbf{d}$ will be FE functions.[1] In this situation, we can clearly reduce the assumptions over these two functions in Theorem 4.1.

The following corollary consists of the restriction of the previous analysis to FE functions.

Corollary 4.2 *Let us assume that $\mathbf{a}_h\in V_h$ and $\mathbf{d}_h\in C_h\cap L^{d+\varepsilon}(\Omega)^d$ for some $\varepsilon>0$. The FE solution of (3.2) satisfies inequality (4.4) for*

$$\xi=1+\frac{h^{\frac{1}{4}}\|\mathbf{a}_h\|_1^{\frac{1}{2}}}{\nu^{\frac{1}{2}}}+\frac{\|\mathbf{d}_h\|_{L^{d+\varepsilon}(\Omega)}}{\sqrt{\nu\lambda}}+\left(1+\frac{\|\mathbf{a}_h\|_1h^{\frac{1}{2}}}{\nu}\right)^{\frac{1}{2}}\left(1+\frac{\|\mathbf{d}_h\|_{L^{d+\varepsilon}(\Omega)}}{\sqrt{\nu\lambda}}\right)^{\frac{1}{2}}. \quad (4.6)$$

Proof: Let us introduce the inequality

$$\|v_h\|_{W_p^l(\Omega)}\lesssim h^{m-l+\frac{d}{p}-\frac{d}{q}}\|v_h\|_{W_q^m(\Omega)} \quad (4.7)$$

[1] In any case, we can always project the continuous fields into the FE spaces using proper projections.

that holds for FE functions v_h, where d is the space dimension (see [17, Th. 4.5.11]). In dimension three, we have that:

$$\tau_1^{\frac{1}{2}}\|\mathbf{a}_h\|_{L^\infty(\Omega)} \lesssim \min(h^{\frac{1}{2}}\|\mathbf{a}_h\|_{L^\infty(\Omega)}^{-\frac{1}{2}}, h\nu^{-\frac{1}{2}})\|\mathbf{a}_h\|_{L^\infty(\Omega)} \lesssim \min\left(h^{\frac{1}{4}}\|\mathbf{a}_h\|_1^{\frac{1}{2}}, h^{\frac{1}{2}}\nu^{-\frac{1}{2}}\|\mathbf{a}_h\|_1\right).$$

Analogously, we obtain:

$$\tau_3^{\frac{1}{2}}(\|\nabla\mathbf{d}_h\|_{L^{d+\varepsilon}(\Omega)} + \|\mathbf{d}_h\|_{L^\infty(\Omega)}) \lesssim \tau_3^{\frac{1}{2}}h^{-1}\|\mathbf{d}_h\|_{L^{d+\varepsilon}(\Omega)} \lesssim \lambda^{-\frac{1}{2}}\|\mathbf{d}_h\|_{L^{d+\varepsilon}(\Omega)},$$

where we have used the inequality (4.7). With regard to the last term in the definition of ξ, we have:

$$\frac{h}{\nu^{\frac{1}{2}}\tau_1^{\frac{1}{2}}} \lesssim \left(1+\frac{\|\mathbf{a}_h\|_1 h^{\frac{1}{2}}}{\nu}\right)^{\frac{1}{2}}\left(1+\frac{\|\mathbf{d}_h\|_{L^{d+\varepsilon}(\Omega)}}{\sqrt{\nu\lambda}}\right)^{\frac{1}{2}}.$$

Therefore, using the fact that $1+\min(a,a^2) \lesssim 1+a$ for any $a>0$, the previous corollary applies for the definition of ξ in (4.6). □

Remark 4.2 In the previous results, we observe that stability bounds for some terms of the Galerkin norm, as well as the extra stability that comes from the stabilization terms do not deteriorate in asymptotic regimes. However, control over $\|p\|$ and $\|\mathbf{b}\|$ can deteriorate for fixed grids in some singular limits of the continuous problem that imply a coercivity loss. Anyway, the same behavior has been observed for the Navier-Stokes problem alone when solved by using stabilized FE techniques.

5 Convergence analysis

Once we have proved stability of the problem, we look at the convergence properties of the numerical algorithm. We are interested in both convergence towards the exact solution (even when it is rough) and optimal order of convergence, i.e. *a priori* error estimates when the solution is smoother.

Using the fact that the stabilized FE problem (3.2) is consistent, i.e. the exact solution satisfies the FE equality, we have that:

$$\begin{aligned}&\mathscr{A}_{\text{stab}}((\chi(\mathbf{u}_h,\mathbf{u}),\chi(\mathbf{b}_h,\mathbf{b}),\chi(p_h,p),\chi(r_h,r)),(\mathbf{v}_h,\mathbf{c}_h,q_h,s_h))\\ &\quad=\mathscr{A}_{\text{stab}}((\varepsilon_h(\mathbf{u}),\varepsilon_h(\mathbf{b}),\varepsilon_h(p),\varepsilon_h(r)),(\mathbf{v}_h,\mathbf{c}_h,q_h,s_h)),\end{aligned}\tag{5.1}$$

where $\chi(v,w) := v-\pi_h(w)$; as stated above, $\varepsilon_h(v) := v-\pi_h(v)$ and $\pi_h(v)$ is a continuous FE interpolant in $H^1(\Omega)$ with optimal interpolation properties that preserves null traces, e.g. the Scott-Zhang interpolant. Let us also define the following norms:

$$\begin{aligned}\|(\mathbf{v},\mathbf{c},q,s)\|_{\widetilde{\text{stab,w}}} &= \nu^{\frac{1}{2}}\|\mathbf{v}\|_1 + \lambda^{\frac{1}{2}}\|\nabla\times\mathbf{c}\| + \|\tau_1^{\frac{1}{2}}X_{\text{u}}(\mathbf{v},q,\mathbf{c})\|_h + \|\tau_2^{\frac{1}{2}}\nabla\cdot\mathbf{v}\|\\ &\quad + \|\tau_3^{\frac{1}{2}}\nabla\times(\mathbf{v}\times\mathbf{d})\| + \|\tau_4^{\frac{1}{2}}\nabla s\|,\\ \|(\mathbf{v},\mathbf{c},q,s)\|_{\widetilde{\text{stab,s}}} &= \frac{\lambda^{\frac{1}{2}}}{L_0}\|\mathbf{c}\| + \frac{1}{\nu^{\frac{1}{2}}}\|q\| + \|(\mathbf{v},\mathbf{c},q,s)\|_{\widetilde{\text{stab,w}}}.\end{aligned}$$

So, the norms with the tilde have all the terms of those without the tilde except the stabilization term related to τ_5. Let us also define the error functions:

$$\begin{aligned}
E_{\mathscr{A}}(h) &:= \tau_1^{-\frac{1}{2}}\|\varepsilon_h(\mathbf{u})\| + \nu^{\frac{1}{2}}\|\nabla\varepsilon_h(\mathbf{u})\| + \lambda^{\frac{1}{2}}\|\varepsilon_h(\mathbf{b})\|_{\mathbf{curl}} \\
&\quad + \min\left\{\nu^{-\frac{1}{2}}L_0^{\frac{1}{2}}\|\mathbf{d}\|_{L^{d+\varepsilon}(\Omega)}\|\nabla\times\varepsilon_h(\mathbf{b})\|, \tau_3^{-\frac{1}{2}}\|\varepsilon_h(\mathbf{b})\|\right\} + \tau_2^{-\frac{1}{2}}\|\varepsilon_h(p)\|, \\
E_{\mathscr{S}}(h) &:= \tau_1^{\frac{1}{2}}\|X_{\mathrm{u}}(\varepsilon_h(\mathbf{u}),\varepsilon_h(p),\varepsilon_h(\mathbf{b})) - \nu\Delta\varepsilon_h(\mathbf{u})\| + \tau_2^{\frac{1}{2}}\|\nabla\cdot\varepsilon_h(\mathbf{u})\| \\
&\quad + \tau_3^{\frac{1}{2}}\|\nabla\times(\varepsilon_h(\mathbf{u})\times\mathbf{d}) + \lambda\nabla\times(\nabla\times\varepsilon_h(\mathbf{b})))\| + \lambda^{\frac{1}{2}}L_0^{-1}\|\varepsilon_h(\mathbf{b})\| \\
&\quad + \lambda^{\frac{1}{2}}L_0^{-1}\left(\sum_{K\in\mathscr{T}_h} h\|\varepsilon_h(\mathbf{b})\|^2_{L^2(\partial K)}\right)^{\frac{1}{2}},
\end{aligned}$$

for some $\varepsilon > 0$. In order for the error function $E_{\mathscr{S}}(h)$ to be well-defined, we require $-\nu\Delta\mathbf{u} + X_{\mathrm{u}}(\mathbf{u},\mathbf{b},p) \in L^2(\Omega)^d$ and $\lambda\nabla\times(\nabla\times\mathbf{b}) - \nabla\times(\mathbf{u}\times\mathbf{d}) \in L^2(\Omega)^d$, which are true for $\mathbf{f}_{\mathrm{u}} \in L^2(\Omega)^d$ and $\mathbf{f}_{\mathrm{b}} \in L^2(\Omega)^d$, respectively; this is easily inferred from the continuous problem. Furthermore, the boundary terms are well defined since $\mathbf{b}_h \in L^2(\partial K)$ for every $K \in \mathscr{T}_h$ (see [6, Corollary 3.8]).

Theorem 5.1 *Under the conditions of Corollary 4.1, the following* a priori *error estimate holds*

$$\|(\mathbf{u}-\mathbf{u}_h, \mathbf{b}-\mathbf{b}_h, p-p_h, r-r_h)\|_{\widetilde{\mathrm{stab,w}}} \lesssim E_{\mathscr{A}}(h) + E_{\mathscr{S}}(h),$$

for the error functions defined above.

Proof: Let us bound the right hand side of the error system (5.1), first Galerkin terms and second stabilization ones. Proceeding as in the proof of Lemma 4.1, we obtain

$$\langle\varepsilon_h(\mathbf{b}), \nabla\times(\mathbf{v}\times\mathbf{d})\rangle \lesssim L_0^{\frac{1}{2}}\|\nabla\times\varepsilon_h(\mathbf{b}_h)\|\|\mathbf{v}\|_1\|\mathbf{d}\|_{L^{d+\varepsilon}(\Omega)}.$$

This result, together with a straight use of integration-by-parts, Schwarz's inequality, the fact that $\varepsilon_h(r) = 0$ and the definition of τ_4, lead to:

$$\begin{aligned}
&\mathscr{A}((\varepsilon_h(\mathbf{u}),\varepsilon_h(\mathbf{b}),\varepsilon_h(p),\varepsilon_h(r)),(\mathbf{v}_h,\mathbf{c}_h,q_h,s_h)) \\
&\quad = -\langle\varepsilon_h(\mathbf{u}), X_{\mathrm{u}}(\mathbf{v}_h,q_h,\mathbf{c}_h)\rangle + \nu(\nabla\varepsilon_h(\mathbf{u}),\nabla\mathbf{v}_h) - (\varepsilon_h(p),\nabla\cdot\mathbf{v}_h) \\
&\qquad + \langle\varepsilon_h(\mathbf{b}),\nabla\times(\mathbf{v}_h\times\mathbf{d})\rangle + \lambda(\nabla\times\varepsilon_h(\mathbf{b}),\nabla\times\mathbf{c}_h) - (\varepsilon_h(\mathbf{b}),\nabla s_h) \\
&\quad \lesssim E_{\mathscr{A}}(h)\|(\mathbf{v}_h,\mathbf{c}_h,q_h,s_h)\|_{\mathrm{stab,w}},
\end{aligned} \tag{5.2}$$

In order to bound the stabilization terms, we proceed as follows:

$$\begin{aligned}
\tau_5(\nabla\cdot\varepsilon_h(\mathbf{b}),\nabla\cdot\mathbf{c}_h) &= \tau_5\sum_{K\in\mathscr{T}_h}\int_K \varepsilon_h(\mathbf{b})\nabla\nabla\cdot\mathbf{c}_h - \tau_5\sum_{K\in\mathscr{T}_h}\int_{\partial K}\mathbf{n}\cdot\varepsilon_h(\mathbf{b})\nabla\cdot\mathbf{c}_h \\
&\lesssim (h^{-1}\tau_5^{\frac{1}{2}}\|\varepsilon_h(\mathbf{b})\| + h^{-\frac{1}{2}}\tau_5^{\frac{1}{2}}\|\varepsilon_h(\mathbf{b})\|_{L^2(\partial K)})\tau_5^{\frac{1}{2}}\|\nabla\cdot\mathbf{c}_h\|.
\end{aligned}$$

where we have used the inequality $\|v\|_{L^2(\partial K)} \leq h^{-\frac{1}{2}}\|v\|_{L^2(K)}$ that holds for FE functions (see [17]). Using the fact that $h^{-1}\tau_5^{\frac{1}{2}} = c_5 L_0^{-1}\lambda^{\frac{1}{2}}$, and Schwarz's inequality we easily obtain:

$$\mathscr{S}(\varepsilon_h(\mathbf{u}),\varepsilon_h(\mathbf{b}),\varepsilon_h(p),\varepsilon_h(r)),(\mathbf{v},\mathbf{c},q,s)) \leq E_{\mathscr{S}}(h)\|(\mathbf{v},\mathbf{c},q,s)\|_{\text{stab,w}}. \tag{5.3}$$

So, using the weak coercivity in Lemma 4.1 and the previous results, we straightforwardly get:

$$\|(\chi(\mathbf{u}_h,\mathbf{u}),\chi(\mathbf{b}_h,\mathbf{b}),\chi(p_h,p),\chi(r_h,r))\|_{\text{stab,w}} \lesssim E_{\mathscr{A}}(h)+E_{\mathscr{S}}(h). \tag{5.4}$$

Finally, using the triangle inequality and the fact that

$$\|(\varepsilon_h(\mathbf{u}),\varepsilon_h(\mathbf{c}),\varepsilon_h(p),\varepsilon_h(s))\|_{\widetilde{\text{stab,w}}} \lesssim E_{\mathscr{A}}(h)+E_{\mathscr{S}}(h)$$

we prove the theorem. □

On the other hand, we can recover convergence on the strong stabilized norm as follows:

Theorem 5.2 *Under the conditions of Corollary 4.2, the following* a priori *error estimate holds*

$$\|(\mathbf{u}-\mathbf{u}_h,\mathbf{b}-\mathbf{b}_h,p-p_h,r-r_h)\|_{\widetilde{\text{stab,s}}} \lesssim \xi(E_{\mathscr{A}}(h)+E_{\mathscr{S}}(h)),$$

for the error functions defined above.

Proof: First, invoking Theorem 4.1, we have

$$\begin{aligned}
&\|(\chi(\mathbf{u}_h,\mathbf{u}),\chi(\mathbf{b}_h,\mathbf{b}),\chi(p_h,p),\chi(r_h,r))\|_{\text{stab,s}} \\
&\lesssim \xi\|(\chi(\mathbf{u}_h,\mathbf{u}),\chi(\mathbf{b}_h,\mathbf{b}),\chi(p_h,p),\chi(r_h,r))\|_{\text{stab,w}} \\
&\quad + \sup_{(\mathbf{v}_h,s_h)\in V_h\times S_h} \frac{\mathscr{A}_{\text{stab}}((\varepsilon_h(\mathbf{u}),\varepsilon_h(\mathbf{b}),\varepsilon_h(p),\varepsilon_h(r)),(\mathbf{v}_h,\mathbf{0},0,s_h))}{\|(\mathbf{v}_h,\mathbf{0},0,s_h)\|_{\text{stab,s}}}.
\end{aligned}$$

We can readily bound the right hand side using the bounds in (5.2)-(5.3) and (5.4), in order to get:

$$\|(\chi(\mathbf{u}_h,\mathbf{u}),\chi(\mathbf{b}_h,\mathbf{b}),\chi(p_h,p),\chi(r_h,r))\|_{\text{stab,s}} \lesssim \xi(E_{\mathscr{A}}(h)+E_{\mathscr{S}}(h)).$$

Using the relation $\tau_2^{-\frac{1}{2}} \lesssim \nu^{-\frac{1}{2}}$ we easily get

$$\|(\varepsilon_h(\mathbf{u}),\varepsilon_h(\mathbf{c}),\varepsilon_h(p),\varepsilon_h(s))\|_{\widetilde{\text{stab,s}}} \lesssim E_{\mathscr{A}}(h)+E_{\mathscr{S}}(h).$$

Combining the last two inequalities and the triangle inequality, we prove the theorem. □

In the asymptotic limit when $h \searrow 0$, we can easily see that

$$\begin{aligned}
E_{\mathscr{A}}(h)+E_{\mathscr{S}}(h) \sim & h^{-1}\|\varepsilon_h(\mathbf{u})\| + \|\varepsilon_h(\mathbf{u})\|_1 + h\|X_{\text{u}}(\varepsilon_h(\mathbf{u}),\varepsilon_h(\mathbf{b}),\varepsilon_h(p)) - \nu\Delta\varepsilon_h(\mathbf{u})\| \\
&+ \|\varepsilon_h(p)\| + \|\varepsilon_h(\mathbf{b})\|_{\mathbf{curl}} + \left(\sum_{K\in\mathscr{T}_h} h\|\varepsilon_h(\mathbf{b})\|^2_{L^2(\partial K)}\right)^{\frac{1}{2}} \\
&+ h\|\nabla\times(\varepsilon_h(\mathbf{u})\times\mathbf{d}) + \lambda\nabla\times(\nabla\times\varepsilon_h(\mathbf{b}))\|.
\end{aligned}$$

So, the convergence results are optimal, in the sense that optimal rates are obtained for smooth enough functions. In order to get convergence to singular components of the magnetic field, the following approximability condition must hold:

$$\lim_{h\to 0}\left\{\|\varepsilon_h(\mathbf{b})\|_{\mathbf{curl}}+\left(\sum_{K\in\mathscr{T}_h} h\|\varepsilon_h(\mathbf{b})\|^2_{L^2(\partial K)}\right)^{\frac{1}{2}}\right\}=0. \tag{5.5}$$

This condition is true for Lagrangian FEs for meshes with a particular macro-element structure (see [6, Assumption 1 and Corollary 5]). One type of element that satisfies this condition is the Powell-Sabin macro-element (see [41,44] and [19, Remark 4.1]); we note that in two space dimensions this macroelement requires its circumcenter to remain inside the FE. Further, numerical experiments in 2D and 3D show that both the Powell-Sabin and *criss-cross* elements provide excellent results (see [7]). In the numerical experiments section, we have extended these results, evaluating the effect of not using this type of meshes in the convergence towards singular solutions. Finally, let us stress the fact that this macro-element structure is only needed for singular solutions, that appear in non-convex domains. For smooth solutions, with $\mathbf{b}\in H^1(\Omega)^d$, the convergence analysis and approximability properties are easy to check and hold for any type of mesh. We refer to [6] for a detailed discussion on this topic, in the framework of the Maxwell operator.

Remark 5.1 It is not the target of the method developed in this work the eigenvalue MHD problem [14]. Since the requirements for a method to be useful for initial and boundary value problems, viz. stability and convergence estimates, are different to the ones for eigenvalue problems (see [12]), it is unclear whether this approach would serve in this last case. However, due to the large amount of problems of interest that are governed by the initial and boundary value MHD problem, efficient methods for this problem, as the one analyzed herein, are useful for the MHD community. We refer to [13] for the application of a similar algorithm to the eigenvalue Maxwell problem.

Remark 5.2 The previous version of the stabilized MHD problem in [21,22] (not converging to singular solutions) has extensively been used for large-scale problems by Shadid and co-workers (see e.g. [43,26]). They have observed that stabilized MHD systems are much easier to solve than inf-sup stable formulations, especially for the parallel algebraic multigrid method in TRILINOS (see [36,37]), and favor their use for large scale MHD problems.

Remark 5.3 This type of stabilized FE formulations have also been used succesfully for transient problems in [8]. It is due to the fact that the divergence-free constraint is explicitly enforced at every time step via the introduction of the pseudo-pressure r.

Remark 5.4 Let us note that a method that introduces similar stabilization terms has been proposed in [13] for electromagnetic eigenvalue problems. The method in [13] depends on a coefficient α and corresponds to the method proposed in [6] for $\alpha=1$ with the only difference that no restriction over the FE spaces or meshes is assumed. Unfortunately, the convergence analysis in [13] does not apply for $\alpha=1$, since the

analysis says that polynomials of infinite order would be required in this case. See [5] and the numerical experiments section for further details.

6 Advection-dominated limits

Applications of the incompressible resisitve MHD simulations in the earth include aluminium electrolysis, electromagnetic pumping, MHD generators, electromagnetic casting and more recently, breeding blankets in fusion reactors. In these applications, the hydrodynamic Reynolds number Re can be high (close to 10^5), which justifies the need to use stabilization techniques. The Hartmann number is usually low (of the order of 1) in most industrial applications. However, some breeding blanket designs in fusion technology involve very large external magnetic fields, leading to Hartmann numbers that can reach 10^5. Finally, the magnetic Reynolds number is low to moderate in all cases, usually in the range $10^{-2}-1$. The dynamo effect in geodynamics deals with moderate magnetic Reynolds number (about 200). Thus, robust FE solvers for industrial (and geophysical) applications should be meaningful in the limit of $\nu \to 0$, whereas the value $\lambda = \mathrm{Ha}^2\mathrm{Re}^{-1}\mathrm{Rm}^{-2}$ is moderate.

Let us note that in these regimes to stabilize the fluid sub-problem is not enough to get error estimates that do not blow up with large hydrodynamic Reynolds numbers. We are forced to stabilize the magnetic sub-problem, in order to treat the term $(-\nabla \times (\varepsilon_h(\mathbf{u}) \times \mathbf{d}), \mathbf{c}_h)$. We refer to [31, Remark 3.5.2] for a detailed explanation of this fact.

Let us discuss the assymptotic behavior of the stabilization parameters related to advection-type stabilization, i.e. τ_1 and τ_3. We consider the non-dimensional equations. Using the simple fact that, given positive values $a,\ b \in \mathbb{R}^+$,

$$\frac{1}{a+b} = \min\{a^{-1}, b^{-1}\}\frac{1}{1+\varepsilon}, \qquad \text{for some } \varepsilon \in [0,1],$$

we can prove, after some algebraic manipulations that

$$\tau_1 \eqsim \min\left\{h, h^2\mathrm{Re}, \frac{\sqrt{\mathrm{Re}}}{\sqrt{h}\mathrm{Ha}}, \frac{1}{h\mathrm{Ha}}\right\},$$
$$\tau_3 \eqsim \min\left\{\frac{h^2\mathrm{Rm}^2\mathrm{Re}}{\mathrm{Ha}^2}, \frac{\sqrt{\mathrm{Re}}}{\sqrt{h}\mathrm{Ha}}, \frac{1}{h\mathrm{Ha}}\right\},$$

where $\eqsim$ stands for equality up to constants. With respect to τ_1, the third and fourth values are of no practical interest, whereas h is the correct value for unresolved areas and $h^2\mathrm{Re}$ is the value in fully resolved regions. On the other hand, the practical value of interest for τ_3 is the first one, whereas the other two prevent τ_3 to blow up for $\mathrm{Rm} \to \infty$. Note that if we let $h \to 0$ the first term will be the minimum even for high Rm numbers.[2] The robustness of the stabilized FE formulation for advection-dominated industrial applications can be found in [31,21,22,43,7].

[2] We note that the continuous problem is singular for $\mathrm{Rm} = \infty$. High magnetic Reynolds numbers appear in astrophysical simulations. However, these simulations always involve transient systems, i.e. the ideal MHD system ($\mathrm{Rm} = \infty$) cannot be stated in steady form. Even though the numerical analysis in this work has been restricted to the steady case for simplicity, the method has been conceived and numerically

7 Some comments on the nonlinear analysis

The numerical analysis of FE methods for the incompressible nonlinear MHD equations is a hard issue; let us recall that this system is obtained taking $(\mathbf{a},\mathbf{d})$ as $(\mathbf{u},\rho\mathbf{b})$ in (2.1). Using inf-sup stable elements, this analysis has been carried out in [42, 32]. It heavily uses the nice properties of Nédélec type FEs and cannot be applied to nodal FEs. For weighted regularization techniques, the full nonlinear analysis has been published in [34]. As stated by the authors, the results in three dimensions are quite restrictive. Finally, a closer formulation to the one presented herein, based on discontinuous Galerkin nodal FEs, is presented in [38]. However, both the numerical analysis and experiments (dealing with singular solutions) are for the linearized problem only. The authors say that the nonlinear extension is an open problem, and up to our knowledge it keeps open so far.

Therefore, the extension of the linearized analysis above to the nonlinear problem is not straightforward. For the nonlinear problem, $\mathbf{a}_h$ and $\mathbf{d}_h$ are in fact the solution of the previous iterate, when using a Picard-type linearization. Thus, we cannot assume regularity over $\mathbf{d}_h$, namely $\mathbf{d}_h \in L^{d+\varepsilon}(\Omega)^d$ for some $\varepsilon > 0$.

We may proceed by induction. Let us denote the iteration counter with a superscript within parentheses. In the nonlinear version of system (2.1) for $i \geq 1$ we replace $\mathbf{a} \leftarrow \mathbf{u}_h^{(i-1)}$, $\mathbf{d} \leftarrow \rho\mathbf{b}_h^{(i-1)}$, and denote the continuous solution of this problem as $(\mathbf{u}^{(i-1)},\mathbf{b}^{(i-1)},p^{(i-1)},r^{(i-1)})$. Next, we obtain the new iterate $(\mathbf{u}_h^{(i)},\mathbf{b}_h^{(i)},p_h^{(i)},r_h^{(i)})$ by solving the discretized problem (3.2). We assume in what follows that the physical properties are such that this iterative scheme converges. Let us also assume that:

$$\mathbf{b}_h^{(i-1)} \text{ is such that } \|\mathbf{b}^{(i-1)} - \mathbf{b}_h^{(i-1)}\| \lesssim h^{\frac{d-2}{2}+\delta^{(i-1)}} \text{ for some } \delta^{(i-1)} > 0 \qquad \text{(A1)}$$

Let us introduce the inverse inequality $\|v_h\|_{L^q(\Omega)} \lesssim h^{\frac{d}{q}-\frac{d}{p}}\|v_h\|_{L^p(\Omega)}$, where $1 \leq p \leq \infty$ and $1 \leq q \leq \infty$ (see [17, Theorem 4.5.11]). We infer that $\|v_h\|_{L^{d+\varepsilon}(\Omega)} \lesssim h^{-\theta_\varepsilon(d)}\|v_h\|$, with $\theta_\varepsilon(2) = \frac{\varepsilon}{2+\varepsilon}$ and $\theta_\varepsilon(3) = \frac{3(1+\varepsilon)}{2(3+\varepsilon)}$ for any $\varepsilon > 0$. Using the stability of the Scott-Zhang projector $\pi_h(\cdot)$, we finally get:

$$\begin{aligned}\|\mathbf{b}_h^{(i-1)}\|_{L^{d+\varepsilon}(\Omega)} &\lesssim \|\pi_h(\mathbf{b}^{(i-1)}) - \mathbf{b}_h^{(i-1)}\|_{L^{d+\varepsilon}(\Omega)} + \|\pi_h(\mathbf{b}^{(i-1)})\|_{L^{d+\varepsilon}(\Omega)} \\ &\lesssim h^{\frac{d-2}{2}+\delta^{(i-1)}-\theta_\varepsilon(d)} + h^{-\theta_\varepsilon(d)}\|\mathbf{b}^{(i-1)} - \pi_h(\mathbf{b}^{(i-1)})\| + \|\mathbf{b}^{(i-1)}\|_{L^{d+\varepsilon}(\Omega)}.\end{aligned}$$

Next, we use the continuous imbedding of $C \cap H(\mathrm{div};\Omega)$ into $H^{\frac{1}{2}+\delta_1}(\Omega)^d$ for some $\delta_1 > 0$ and the interpolation properties of the Scott-Zhang projector (see [17, Theorem 4.8.12]) to infer that $\|\mathbf{b}^{(i-1)} - \pi_h(\mathbf{b}^{(i-1)})\| \lesssim h^{\frac{1}{2}+\delta_1}\|\mathbf{b}^{(i-1)}\|_{\mathbf{curl}}$ On the other hand, since $C \cap H(\mathrm{div};\Omega)$ is compactly imbedded into $L^{3+\delta_2}(\Omega)$, for some $\delta_2 > 0$ (see [42, Proposition 2.3] and [1, Proposition 3.7]), we can pick an $\varepsilon = \varepsilon(\delta^{(i-1)},\delta_1,\delta_2) > 0$ small enough such that $\|\mathbf{b}_h^{(i-1)}\|_{L^{d+\varepsilon}(\Omega)} \lesssim \|\mathbf{b}^{(i-1)}\|_{\mathbf{curl}}$.

tested for the transient problem [7]. The first value in τ_3 does not blow up for $\mathrm{Rm} = \infty$ when applied to transient problem, since it will include a time-step size δt dependency when using a quasi-static approach or a dynamic subgrid stabilization will be used (see [23] for details).

From Theorem 5.2, we have that $\|\mathbf{b}^{(i)} - \mathbf{b}_h^{(i)}\| \lesssim \xi(E_{\mathscr{A}}(h) + E_{\mathscr{S}}(h))$, where ξ is now bounded. Assuming that:

$$E_{\mathscr{A}}(h) + E_{\mathscr{S}}(h) \lesssim h^{\frac{d-2}{2}+\delta^{(i)}} \text{ for some } \delta^{(i)} > 0, \tag{A2}$$

we finally obtain that $\|\mathbf{b}^{(i)} - \mathbf{b}_h^{(i)}\| \lesssim h^{\frac{1}{2}+\delta^{(i)}}$.

Assumption A1 is easily satisfied. In fact, we only need to start the process with a $\mathbf{b}_h^{(0)} \in C \cap H(\mathrm{div};\Omega)$, e.g. $\mathbf{b}_h^{(0)} = \mathbf{0}$ and $\mathbf{b}^{(0)} = \mathbf{0}$, so that the effective initial guess is a solution of a linear problem for which we know that A1 holds [6].

Assumption A2 is true for $(\mathbf{u}^{(i-1)}, p^{(i-1)}) \in H^{\frac{d}{2}+\varepsilon}(\Omega)^d \times H^{\frac{d-2}{2}+\varepsilon}(\Omega)$; the terms related to $\mathbf{b}$ can be treated as in [6, Corollary 3.12]. In dimension three, it requires $(\mathbf{u}^{(i-1)}, p^{(i-1)}) \in H^{\frac{3}{2}+\varepsilon}(\Omega)^d \times H^{\frac{1}{2}+\varepsilon}(\Omega)$ for an arbitrary small $\varepsilon > 0$.

8 Numerical experimentation

The objective of the following numerical experiment is to compare the approximation of singular solutions for the MHD problem using several mesh structures. We will show the difference between a mesh with a suitable macro-element structure, the crossbox element, which has been observed numerically that verifies the approximability condition (5.5), against mesh structures that do not satisfy it, both in terms of convergence rates and the solution itself.

The chosen problem with non-smooth solution corresponds to solve the MHD equations in a nonconvex L-shaped domain $\Omega = (-1,1)\times(-1,1)\setminus[0,1]\times[0,-1]$. Both the hydrodynamic and magnetic solutions have strong singularities at the reentrant corner, where the origin of coordinates is taken. The singular solution for the Stokes operator is described in polar coordinates (r,θ) by

$$\begin{aligned}
u_x(x,y) &= r^{\lambda}\left((1+\lambda)\sin(\theta)\psi(\theta) + \cos(\theta)\psi'(\theta)\right),\\
u_y(x,y) &= r^{\lambda}\left(-(1+\lambda)\cos(\theta)\psi(\theta) + \sin(\theta)\psi'(\theta)\right),\\
p(x,y) &= -\frac{r^{\lambda-1}}{1-\lambda}\left((1+\lambda)^2\psi'(\theta) + \psi'''(\theta)\right),
\end{aligned}$$

where

$$\begin{aligned}
\psi(\theta) = &\sin((1+\lambda)\theta)\frac{\cos(\lambda\omega)}{1+\lambda} - \cos((1+\lambda)\theta)\\
&- \sin((1-\lambda)\theta)\frac{\cos(\lambda\omega)}{1-\lambda} + \cos((1-\lambda)\theta).
\end{aligned}$$

The value of the parameter λ is the smallest positive solution of

$$\sin(\lambda\omega) + \lambda\sin(\omega) = 0, \quad \text{where } \omega = \frac{3\pi}{2},$$

which is $\lambda \sim 0.54448373678246$. Note that $\mathbf{u} = (u_x, u_y)$ is solenoidal and $(\mathbf{u}, p) \in H^{1+\lambda}(\Omega)^2 \times H^{\lambda}(\Omega)$.

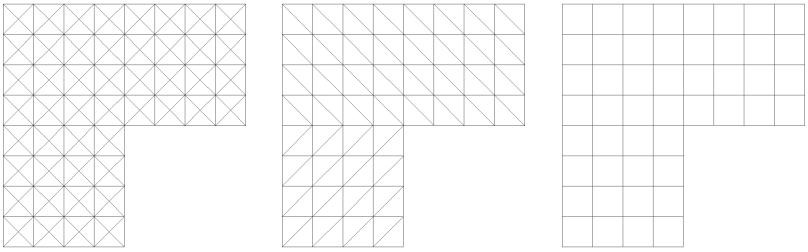

(a) Crossbox element (b) P1 element (c) Q1 element

Fig. 8.1 The three topologies of meshes used for the numerical experiments for a characteristic element size $h = 2^{-2}$.

The singular solution for the Maxwell operator is defined, also in polar coordinates, as

$$\mathbf{b}(x,y) = \nabla\left(r^{\frac{2n}{3}}\sin\left(\frac{2n}{3}\right)\right), \qquad n \in \mathbb{N}^+.$$

Note that $\nabla\cdot\mathbf{b} = 0$ and $\nabla\times\mathbf{b} = \mathbf{0}$. The magnetic induction field $\mathbf{b} \in H^{\frac{2n}{3}}(\Omega)^2$ and therefore, $\mathbf{b} \notin H^1(\Omega)^2$ for $n = 1$.

This problem has been solved using several mesh structures. On one hand, we have used meshes with a macro-element structure, namely the crossbox element, which satisfies the approximability condition (5.5). On the other hand, we have used meshes composed of linear elements, both triangular meshes (P1) and quadrilateral meshes (Q1) that do not verify (5.5). Figure 8.1 shows an example of the three different mesh structures for $h = 2^{-2}$. Moreover, let us stress that we have solved the problem fully coupled with a nonlinear tolerance of 10^{-4} and setting every physical parameter to 1.

For the three cases, the problem has been solved in several meshes with different mesh sizes, from the coarsest one with $h = 2^{-2}$ to the finest one with $h = 2^{-10}$, which consists of 12,58 million elements for the mesh composed of crossbox elements. Tables 8.1-8.6 contain the numerical error norms of the hydrodynamical and magnetic variables for the three cases, crossbox, P1 and Q1 elements respectively. In Tables 8.1, 8.3 and 8.5, related to the hydrodynamical variables, we show the numerical errors for the velocity in the L^2-norm and the H^1-norm, and the error for the pressure in the L^2-norm. In Tables 8.2, 8.4 and 8.6, related to the magnetic unknowns, we have listed the numerical errors for the magnetic induction in the L^2-norm and the $H(\mathbf{curl})$-norm, and the errors for the magnetic pseudo-pressure in both the L^2-norm and the H^1-norm. Furthermore, Figure 8.2 shows the convergence plots of the computed numerical errors. It is clearly seen that using a mesh with a macro-element structure is crucial in order to obtain the theoretical convergence rates to singular solutions. It is also shown that linear elements, both P1 and Q1 meshes, have a much lower convergence rate.

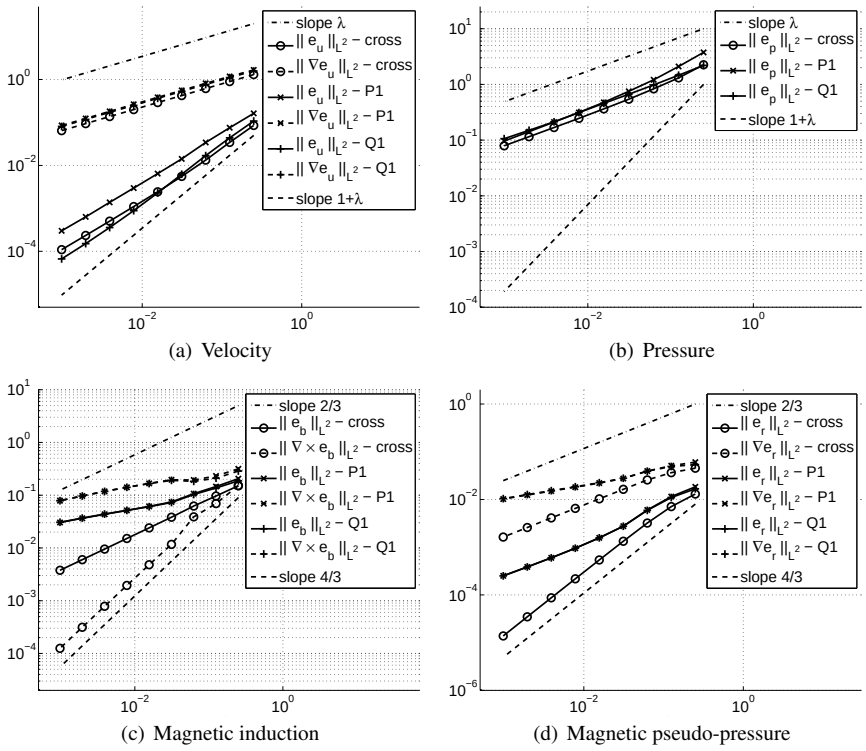

(a) Velocity (b) Pressure

(c) Magnetic induction (d) Magnetic pseudo-pressure

Fig. 8.2 Convergence plots for *h*-refinement. Results for velocity, pressure, magnetic induction and magnetic pseudo-pressure and the three different meshes.

However, when using meshes of linear elements, both P1 and Q1, the method provides a solution for the magnetic induction **b** with spurious discontinuities around the corner. Figure 8.3 displays the magnetic induction solution for the three different mesh structures. Besides, Figure 8.4 shows a zoom of the same magnetic induction fields around the corner in order to highlight the discontinuities that appear when computing with meshes that do not satisfy condition (5.5).

Finally, we observe that 1) the convergence rates for $\|\nabla \mathbf{e}_{\mathrm{u}}\|$, $\|e_p\|$, $\|\mathbf{e}_{\mathrm{b}}\|$ and $\|\nabla e_r\|$ are *exactly* those predicted by the numerical analysis of the uncoupled stabilized Stokes and Maxwell problems, 2) super-convergence is observed for the error quantities $\|\mathbf{e}_{\mathrm{u}}\|$ and $\|\nabla \times \mathbf{e}_{\mathrm{b}}\|$. In fact, we can infer from the numerical analysis that the error due to the coupling term is affected by the two quantities that exhibit super-convergence. As a result, the coupling terms are small compared to those related to the uncoupled fluid and magnetic sub-problems, leading to the first observation.

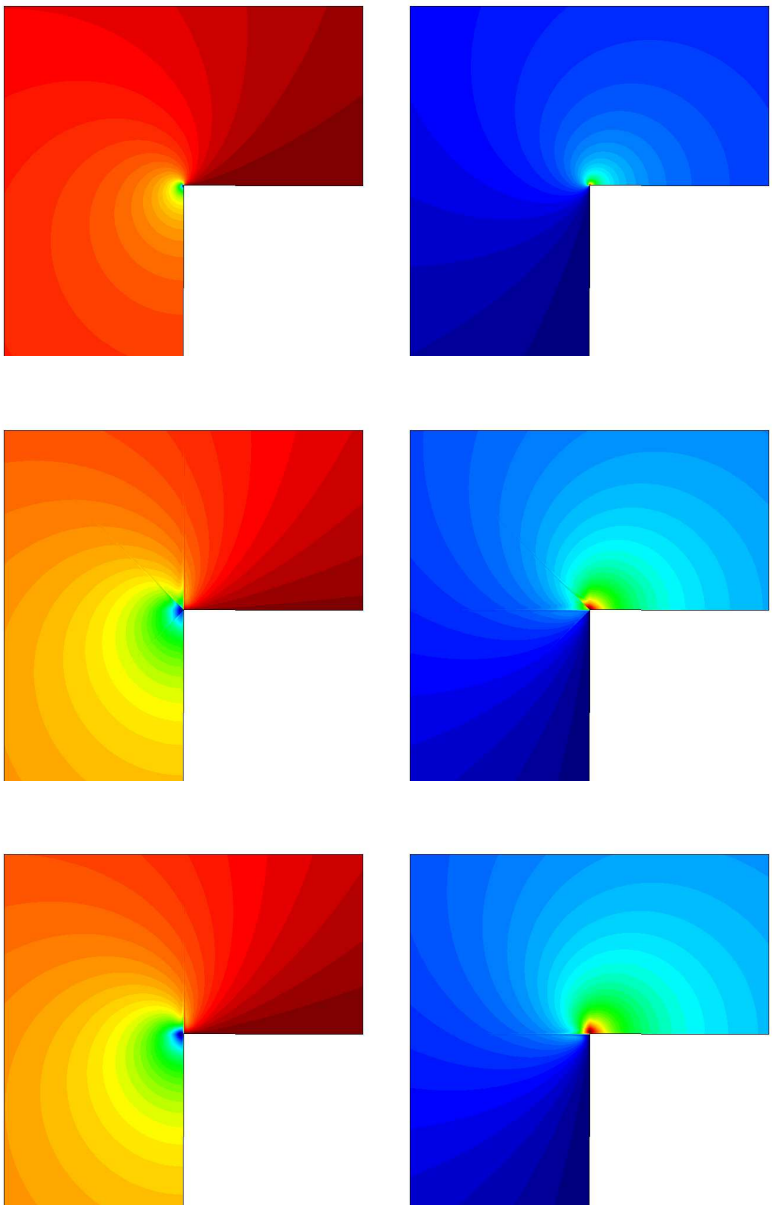

Fig. 8.3 Magnetic induction solution for $h = 2^{-8}$. x-component (left) and y-component (right). Crossbox (top), P1 (middle) and Q1 (bottom) elements.

h	$\|\|\mathbf{e}_\mathrm{u}\|\|$	$\|\|\nabla\mathbf{e}_\mathrm{u}\|\|$	$\|\|e_p\|\|$
2^{-2}	$8.52\cdot10^{-2}$ (-)	$1.30\cdot10^{0}$ (-)	$2.25\cdot10^{0}$ (-)
2^{-3}	$3.43\cdot10^{-2}$ (1.31)	$8.96\cdot10^{-1}$ (0.54)	$1.31\cdot10^{0}$ (0.78)
2^{-4}	$1.33\cdot10^{-2}$ (1.37)	$6.17\cdot10^{-1}$ (0.54)	$8.34\cdot10^{-1}$ (0.65)
2^{-5}	$5.54\cdot10^{-3}$ (1.26)	$4.23\cdot10^{-1}$ (0.54)	$5.42\cdot10^{-1}$ (0.62)
2^{-6}	$2.43\cdot10^{-3}$ (1.19)	$2.91\cdot10^{-1}$ (0.54)	$3.63\cdot10^{-1}$ (0.58)
2^{-7}	$1.10\cdot10^{-3}$ (1.14)	$1.99\cdot10^{-1}$ (0.55)	$2.46\cdot10^{-1}$ (0.56)
2^{-8}	$5.04\cdot10^{-4}$ (1.13)	$1.37\cdot10^{-1}$ (0.54)	$1.68\cdot10^{-1}$ (0.55)
2^{-9}	$2.34\cdot10^{-4}$ (1.11)	$9.40\cdot10^{-2}$ (0.54)	$1.15\cdot10^{-1}$ (0.55)
2^{-10}	$1.09\cdot10^{-4}$ (1.10)	$6.44\cdot10^{-2}$ (0.55)	$7.89\cdot10^{-2}$ (0.54)

Table 8.1 Numerical errors for hydrodynamic unknowns and rate of convergence in brackets. Crossbox element.

h	$\|\|\mathbf{e}_\mathrm{b}\|\|$	$\|\|\nabla\times\mathbf{e}_\mathrm{b}\|\|$	$\|\|e_r\|\|$	$\|\|\nabla e_r\|\|$
2^{-2}	$1.51\cdot10^{-1}$ (-)	$1.52\cdot10^{-1}$ (-)	$1.30\cdot10^{-2}$ (-)	$4.52\cdot10^{-2}$ (-)
2^{-3}	$9.66\cdot10^{-2}$ (0.64)	$6.94\cdot10^{-2}$ (1.13)	$7.08\cdot10^{-3}$ (0.88)	$3.64\cdot10^{-2}$ (0.31)
2^{-4}	$6.22\cdot10^{-2}$ (0.64)	$3.89\cdot10^{-2}$ (0.84)	$3.21\cdot10^{-3}$ (1.14)	$2.57\cdot10^{-2}$ (0.50)
2^{-5}	$3.83\cdot10^{-2}$ (0.70)	$1.17\cdot10^{-2}$ (1.73)	$1.33\cdot10^{-3}$ (1.27)	$1.63\cdot10^{-2}$ (0.66)
2^{-6}	$2.40\cdot10^{-2}$ (0.67)	$4.80\cdot10^{-3}$ (1.29)	$5.39\cdot10^{-4}$ (1.30)	$1.03\cdot10^{-2}$ (0.66)
2^{-7}	$1.51\cdot10^{-2}$ (0.67)	$1.95\cdot10^{-3}$ (1.30)	$2.17\cdot10^{-4}$ (1.31)	$6.50\cdot10^{-3}$ (0.66)
2^{-8}	$9.51\cdot10^{-3}$ (0.67)	$7.83\cdot10^{-4}$ (1.32)	$8.69\cdot10^{-5}$ (1.32)	$4.10\cdot10^{-3}$ (0.66)
2^{-9}	$5.99\cdot10^{-3}$ (0.67)	$3.14\cdot10^{-4}$ (1.32)	$3.47\cdot10^{-5}$ (1.32)	$2.58\cdot10^{-3}$ (0.67)
2^{-10}	$3.77\cdot10^{-3}$ (0.67)	$1.25\cdot10^{-4}$ (1.33)	$1.38\cdot10^{-5}$ (1.33)	$1.63\cdot10^{-3}$ (0.66)

Table 8.2 Numerical errors for magnetic unknowns and rate of convergence in brackets. Crossbox element.

h	$\|\|\mathbf{e}_\mathrm{u}\|\|$	$\|\|\nabla\mathbf{e}_\mathrm{u}\|\|$	$\|\|e_p\|\|$
2^{-2}	$1.63\cdot10^{-1}$ (-)	$1.67\cdot10^{0}$ (-)	$3.76\cdot10^{0}$ (-)
2^{-3}	$7.55\cdot10^{-2}$ (1.11)	$1.18\cdot10^{0}$ (0.50)	$2.10\cdot10^{0}$ (0.84)
2^{-4}	$3.42\cdot10^{-2}$ (1.14)	$8.14\cdot10^{-1}$ (0.54)	$1.21\cdot10^{0}$ (0.80)
2^{-5}	$1.42\cdot10^{-2}$ (1.27)	$5.59\cdot10^{-1}$ (0.54)	$7.51\cdot10^{-1}$ (0.69)
2^{-6}	$6.43\cdot10^{-3}$ (1.14)	$3.84\cdot10^{-1}$ (0.54)	$4.77\cdot10^{-1}$ (0.65)
2^{-7}	$2.97\cdot10^{-3}$ (1.11)	$2.64\cdot10^{-1}$ (0.54)	$3.14\cdot10^{-1}$ (0.60)
2^{-8}	$1.38\cdot10^{-3}$ (1.11)	$1.81\cdot10^{-1}$ (0.54)	$2.11\cdot10^{-1}$ (0.57)
2^{-9}	$6.34\cdot10^{-4}$ (1.12)	$1.24\cdot10^{-1}$ (0.55)	$1.42\cdot10^{-1}$ (0.57)
2^{-10}	$3.00\cdot10^{-4}$ (1.08)	$8.53\cdot10^{-2}$ (0.54)	$9.61\cdot10^{-2}$ (0.56)

Table 8.3 Numerical errors for hydrodynamic unknowns and rate of convergence in brackets. P1 element.

h	$\|\|\mathbf{e}_b\|\|$	$\|\|\nabla\times\mathbf{e}_b\|\|$	$\|\|e_r\|\|$	$\|\|\nabla e_r\|\|$
2^{-2}	$2.06\cdot10^{-1}$ (-)	$3.16\cdot10^{-1}$ (-)	$1.84\cdot10^{-2}$ (-)	$6.06\cdot10^{-2}$ (-)
2^{-3}	$1.46\cdot10^{-1}$ (0.50)	$2.32\cdot10^{-1}$ (0.45)	$1.15\cdot10^{-2}$ (0.68)	$5.11\cdot10^{-2}$ (0.25)
2^{-4}	$1.07\cdot10^{-1}$ (0.45)	$1.94\cdot10^{-1}$ (0.26)	$6.04\cdot10^{-3}$ (0.93)	$3.94\cdot10^{-2}$ (0.38)
2^{-5}	$7.44\cdot10^{-2}$ (0.52)	$1.96\cdot10^{-1}$ (-0.01)	$2.76\cdot10^{-3}$ (1.13)	$2.75\cdot10^{-2}$ (0.52)
2^{-6}	$6.13\cdot10^{-2}$ (0.28)	$1.67\cdot10^{-1}$ (0.23)	$1.57\cdot10^{-3}$ (0.81)	$2.21\cdot10^{-2}$ (0.32)
2^{-7}	$5.16\cdot10^{-2}$ (0.25)	$1.41\cdot10^{-1}$ (0.24)	$9.51\cdot10^{-4}$ (0.72)	$1.81\cdot10^{-2}$ (0.29)
2^{-8}	$4.35\cdot10^{-2}$ (0.25)	$1.18\cdot10^{-1}$ (0.26)	$5.98\cdot10^{-4}$ (0.67)	$1.50\cdot10^{-2}$ (0.27)
2^{-9}	$3.65\cdot10^{-2}$ (0.25)	$9.68\cdot10^{-2}$ (0.29)	$3.85\cdot10^{-4}$ (0.64)	$1.24\cdot10^{-2}$ (0.27)
2^{-10}	$3.04\cdot10^{-2}$ (0.26)	$7.89\cdot10^{-2}$ (0.29)	$2.51\cdot10^{-4}$ (0.62)	$1.02\cdot10^{-2}$ (0.28)

Table 8.4 Numerical errors for magnetic unknowns and rate of convergence in brackets. P1 element.

h	$\|\|\mathbf{e}_u\|\|$	$\|\|\nabla\mathbf{e}_u\|\|$	$\|\|e_p\|\|$
2^{-2}	$1.08\cdot10^{-1}$ (-)	$1.58\cdot10^{0}$ (-)	$2.19\cdot10^{0}$ (-)
2^{-3}	$4.39\cdot10^{-2}$ (1.30)	$1.11\cdot10^{0}$ (0.51)	$1.46\cdot10^{0}$ (0.58)
2^{-4}	$1.69\cdot10^{-2}$ (1.38)	$7.67\cdot10^{-1}$ (0.53)	$9.80\cdot10^{-1}$ (0.58)
2^{-5}	$6.23\cdot10^{-3}$ (1.44)	$5.29\cdot10^{-1}$ (0.54)	$6.67\cdot10^{-1}$ (0.56)
2^{-6}	$2.29\cdot10^{-3}$ (1.44)	$3.64\cdot10^{-1}$ (0.54)	$4.57\cdot10^{-1}$ (0.55)
2^{-7}	$8.82\cdot10^{-4}$ (1.38)	$2.50\cdot10^{-1}$ (0.54)	$3.12\cdot10^{-1}$ (0.55)
2^{-8}	$3.57\cdot10^{-4}$ (1.30)	$1.72\cdot10^{-1}$ (0.54)	$2.13\cdot10^{-1}$ (0.55)
2^{-9}	$1.51\cdot10^{-4}$ (1.24)	$1.18\cdot10^{-1}$ (0.54)	$1.50\cdot10^{-1}$ (0.51)
2^{-10}	$6.66\cdot10^{-5}$ (1.18)	$8.08\cdot10^{-2}$ (0.55)	$1.06\cdot10^{-1}$ (0.50)

Table 8.5 Numerical errors for hydrodynamic unknowns and rate of convergence in brackets. Q1 element.

h	$\|\|\mathbf{e}_b\|\|$	$\|\|\nabla\times\mathbf{e}_b\|\|$	$\|\|e_r\|\|$	$\|\|\nabla e_r\|\|$
2^{-2}	$1.87\cdot10^{-1}$ (-)	$2.87\cdot10^{-1}$ (-)	$1.67\cdot10^{-2}$ (-)	$5.38\cdot10^{-2}$ (-)
2^{-3}	$1.37\cdot10^{-1}$ (0.45)	$2.10\cdot10^{-1}$ (0.45)	$1.10\cdot10^{-2}$ (0.60)	$4.92\cdot10^{-2}$ (0.13)
2^{-4}	$1.03\cdot10^{-1}$ (0.41)	$1.83\cdot10^{-1}$ (0.20)	$5.91\cdot10^{-3}$ (0.90)	$3.92\cdot10^{-2}$ (0.33)
2^{-5}	$7.27\cdot10^{-2}$ (0.50)	$1.91\cdot10^{-1}$ (-0.06)	$2.75\cdot10^{-3}$ (1.10)	$2.79\cdot10^{-2}$ (0.49)
2^{-6}	$6.06\cdot10^{-2}$ (0.26)	$1.66\cdot10^{-1}$ (0.20)	$1.57\cdot10^{-3}$ (0.81)	$2.25\cdot10^{-2}$ (0.31)
2^{-7}	$5.15\cdot10^{-2}$ (0.23)	$1.41\cdot10^{-1}$ (0.24)	$9.50\cdot10^{-4}$ (0.72)	$1.85\cdot10^{-2}$ (0.28)
2^{-8}	$4.38\cdot10^{-2}$ (0.23)	$1.18\cdot10^{-1}$ (0.26)	$5.98\cdot10^{-4}$ (0.67)	$1.53\cdot10^{-2}$ (0.27)
2^{-9}	$3.69\cdot10^{-2}$ (0.25)	$9.66\cdot10^{-2}$ (0.29)	$3.85\cdot10^{-4}$ (0.64)	$1.27\cdot10^{-2}$ (0.27)
2^{-10}	$3.07\cdot10^{-2}$ (0.27)	$7.86\cdot10^{-2}$ (0.30)	$2.50\cdot10^{-4}$ (0.62)	$1.04\cdot10^{-2}$ (0.29)

Table 8.6 Numerical errors for magnetic unknowns and rate of convergence in brackets. Q1 element.

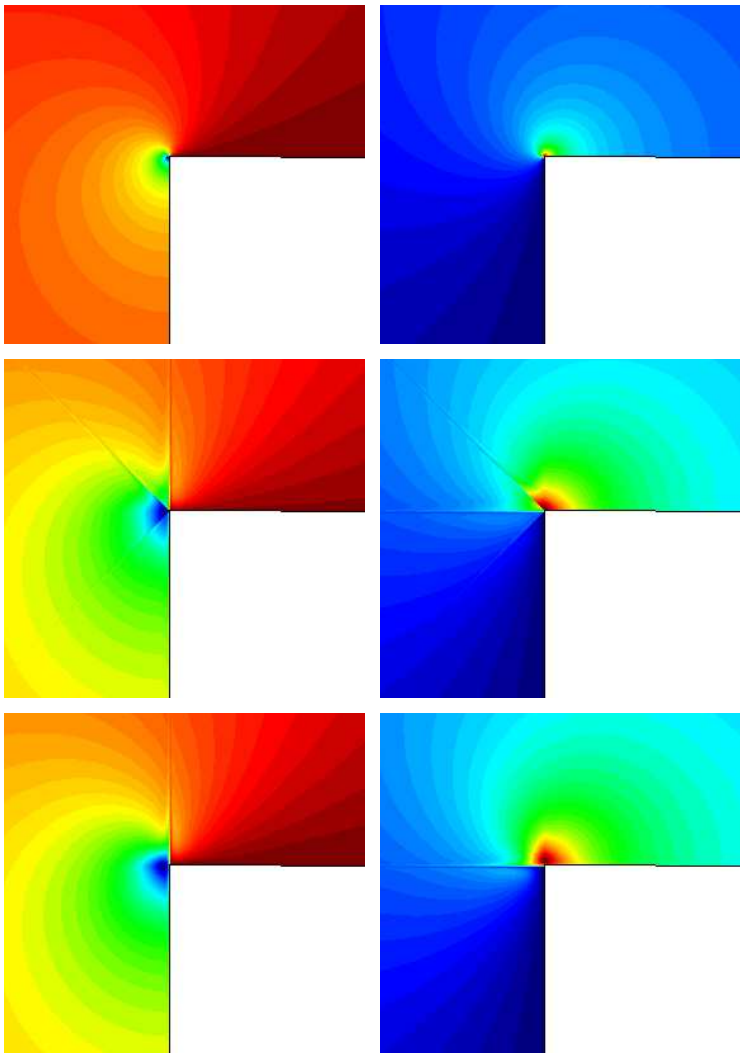

Fig. 8.4 Zoom of the magnetic induction solution for $h = 2^{-8}$ around the corner. x-component (left) and y-component (right). Crossbox (top), P1 (middle) and Q1 (bottom) elements.

9 Conclusions

The finite element approximation of the resistive MHD problem in [7] has been analyzed in this work. The formulation falls within the category of stabilized finite element methods and, as such, is intended to avoid the need for using finite element approximations satisfying the compatibility conditions of the continuous problem and dealing with ranges of the physical parameters in which first order derivatives dominate second order ones.

Particular features of the formulation analyzed are that it is of residual type, can be based on the VMS framework and the stabilization parameters are designed from the numerical analysis, accounting for the coupling between the fluid and magnetic subproblems. However, the most salient feature is that it allows to converge to singular solutions even when using a continuous Lagrangian approximation for the magnetic induction field. To our knowledge, this is the first time this is achieved. From the technical point of view, this possibility relies on the fact that we mimic the correct functional setting of the continuous problem at the discrete level.

The stability and convergence analysis in this work support the feasibility of our formulation, and complements the numerical experimentation in [7]. We have restricted ourselves to some simplifying assumptions (quasi-uniform meshes, constant stabilization parameters, conforming finite element spaces) which have allowed us to avoid excessive technicalities but to highlight the main analytical reasons for the success of our formulation.[3]

References

1. C. Amrouche, C. Bernardi, M. Dauge, and V. Girault. Vector potentials in three-dimensional non-smooth domains. *Mathematical Methods in the Applied Sciences*, 21(9):823–864, 1998.
2. F. Armero and J. C. Simo. Long-term dissipativity of time-stepping algorithms for an abstract evolution equation with applications to the incompressible MHD and Navier-Stokes equations. *Computer Methods in Applied Mechanics and Engineering*, 131(1-2):41 – 90, 1996.
3. S. H. Aydın, A. I. Nesliturk, and M. Tezer-Sezgin. Two-level finite element method with a stabilizing subgrid for the incompressible MHD equations. *International Journal for Numerical Methods in Fluids*, 62(2):188–210, 2010.
4. S. Badia and R. Codina. Unified stabilized finite element formulations for the Stokes and the Darcy problems. *SIAM Journal on Numerical Analysis*, 47(3):1977–2000, 2009.
5. S. Badia and R. Codina. A combined nodal continuous–discontinuous finite element formulation for the Maxwell problem. *Applied Mathematics and Computation*, 218(8):4276–4294, 2011.
6. S. Badia and R. Codina. A nodal-based finite element approximation of the Maxwell problem suitable for singular solutions. *SIAM Journal on Numerical Analysis*, 50(2):398–417, 2012.
7. S. Badia, R. Codina, and R. Planas. On an unconditionally convergent stabilized finite element approximation of resistive magnetohydrodynamics. *Journal of Computational Physics*, 234:399–416, 2013.
8. S. Badia, R. Planas, and J. V. Gutiérrez-Santacreu. Unconditionally stable operator splitting algorithms for the incompressible magnetohy drodynamics system discretized by a stabilized finite element formulation based on projections. *International Journal for Numerical Methods in Engineering*, 93(3):302–328, 2013.
9. M. A. Belenli, S. Kaya, L. G. Rebholz, and N. E. Wilson. A subgrid stabilization finite element method for incompressible magnetohydrodynamics. *International Journal of Computer Mathematics*, pages 1–18, in press.
10. N. Ben Salah, A. Soulaimani, and W.G. Habashi. A finite element method for magnetohydrodynamics. *Computer Methods in Applied Mechanics and Engineering*, 190(43-44):5867 – 5892, 2001.
11. N. Ben Salah, A. Soulaimani, W.G. Habashi, and M. Fortin. A conservative stabilized finite element method for the magneto-hydrodynamic equations. *International Journal for Numerical Methods in Fluids*, 29(5):535–554, 1999.
12. D. Boffi. Finite element approximation of eigenvalue problems. *Acta Numerica*, 19:1–120, 2010.
13. A. Bonito and J. Guermond. Approximation of the eigenvalue problem for the time harmonic Maxwell system by continuous Lagrange finite elements. *Mathematics of Computation*, 80:1887–1910, 2011.

[3] The analysis for non-degenerate meshes and variable stabilization parameters introduces some additional technicalities. We refer to [20,4] for the numerical analysis of stabilized FE discretizations of Navier-Stokes and Maxwell problems respectively, in this more general setting.

14. L. Boulton and M. Strauss. Eigenvalue enclosures and convergence for the linearized MHD operator. *BIT Numerical Mathematics*, 52(4):801–825, 2012.
15. J. H. Bramble, T. V. Kolev, and J. E. Pasciak. The approximation of the Maxwell eigenvalue problem using a least-squares method. *Mathematics of Computation*, 74(252):1575–1598, 2005.
16. J. H. Bramble and J. E. Pasciak. A new approximation technique for div-curl systems. *Mathematics of Computation*, 73(248):1739–1762, 2004.
17. S.C. Brenner and L.R. Scott. *The Mathematical Theory of Finite Element Methods*. Springer–Verlag, 1994.
18. F. Brezzi and M. Fortin. *Mixed and Hybrid Finite Element Methods*. Springer Verlag, 1991.
19. A. Buffa, P. Ciarlet Jr., and E. Jamelot. Solving electromagnetic eigenvalue problems in polyhedral domains with nodal finite elements. *Numerische Mathematik*, 113(4):497–518, 2009.
20. R. Codina. Analysis of a stabilized finite element approximation of the Oseen equations using orthogonal subscales. *Applied Numerical Mathematics*, 58:264–283, 2008.
21. R. Codina and N. Hernández. Stabilized finite element approximation of the stationary MHD equations. *Computational Mechanics*, 38:344–355, 2006.
22. R. Codina and N. Hernández. Approximation of the thermally coupled MHD problem using a stabilized finite element method. *Journal of Computational Physics*, 230(4):1281 – 1303, 2011.
23. R. Codina, J. Principe, O. Guasch, and S. Badia. Time dependent subscales in the stabilized finite element approximation of incompressible flow problems. *Computer Methods in Applied Mechanics and Engineering*, 196(21-24):2413 – 2430, 2007.
24. M. Costabel. A coercive bilinear form for Maxwell's equations. *Journal of Mathematical Analysis and Applications*, 157(2):527–541, 1991.
25. M. Costabel and M. Dauge. Weighted regularization of Maxwell equations in polyhedral domains. *Numerische Mathematik*, 93(2):239–277, 2002.
26. E. C. Cyr, J. N Shadid, R. S. Tuminaro, R. P. Pawlowski, and L. Chacón. A new approximate block factorization preconditioner for two-dimensional incompressible (reduced) resistive MHD. *SIAM Journal on Scientific Computing*, 35(3):B701–B730, 2013.
27. P.A. Davidson. *An introduction to magnetohydrodynamics*. Cambridge University Press, 2001.
28. H.-Y. Duan, F. Jia, P. Lin, and R. C. E. Tan. The local L^2 projected C^0 finite element method for Maxwell problem. *SIAM Journal on Numerical Analysis*, 47(2):1274–1303, 2009.
29. A. Ern and J.L. Guermond. *Theory and Practice of Finite Elements*. Springer–Verlag, 2004.
30. J.-F. Gerbeau. A stabilized finite element method for the incompressible magnetohydrodynamic equations. *Numerische Mathematik*, 87:83–111, 2000.
31. J.F. Gerbeau, C. Le Bris, and T. Lelièvre. *Mathematical methods for the magnetohydrodynamics of liquid metals*. Oxford University Press, USA, 2006.
32. C. Greif, D. Li, D. Schotzau, and X. Wei. A mixed finite element method with exactly divergence-free velocities for incompressible magnetohydrodynamics. *Computer Methods in Applied Mechanics and Engineering*, 199(45–48):2840–2855, 2010.
33. M.D. Gunzburger, A.J. Meir, and J.P. Peterson. On the existence, uniqueness, and finite element approximation of solutions of the equations of stationary, incompressible magnetohydrodynamics. *Math. Comp.*, 56:523–563, 1991.
34. U. Hasler, A. Schneebeli, and D. Schötzau. Mixed finite element approximation of incompressible MHD problems based on weighted regularization. *Applied Numerical Mathematics*, 51:19 – 45, 2004.
35. C. Hazard and M. Lenoir. On the solution of time-harmonic scattering problems for Maxwell's equations. *SIAM Journal on Mathematical Analysis*, 27(6):1597–1630, 1996.
36. M. A. Heroux, R. A. Bartlett, V. E. Howle, R. J. Hoekstra, J. J. Hu, T. G. Kolda, R. B. Lehoucq, K. R. Long, R. P. Pawlowski, E. T. Phipps, A. G. Salinger, H. K. Thornquist, R. S. Tuminaro, J. M. Willenbring, A. Williams, and K. S. Stanley. An overview of the Trilinos project. *ACM Transactions on Mathematical Software*, 31(3):397–423, 2005.
37. M. A. Heroux and J. M. Willenbring. Trilinos users guide. Technical Report SAND2003-2952, Sandia National Laboratories, 2003.
38. P. Houston, D. Schötzau, and X. Wei. A mixed DG method for linearized incompressible magnetohydrodynamics. *Journal of Scientific Computing*, 40:281–314, 2009.
39. P.-W. Hsieh and S.-Y. Yang. A bubble-stabilized least-squares finite element method for steady MHD duct flow problems at high hartmann numbers. *Journal of Computational Physics*, 228:8301–8320, 2009.
40. P. Monk. *Finite Element Methods for Maxwell's Equations*. Oxford University Press, 2003.
41. M. J. D. Powell and M. A. Sabin. Piecewise quadratic approximations on triangles. *ACM Trans. Math. Softw.*, 3(4):316–325, 1977.

42. D. Schötzau. Mixed finite element methods for stationary incompressible magneto-hydrodynamics. *Numerische Mathematik*, 96:771–800, 2004.
43. J.N. Shadid, R.P. Pawlowski, J.W. Banks, L. Chacon, P.T. Lin, and R.S. Tuminaro. Towards a scalable fully-implicit fully-coupled resistive MHD formulation with stabilized FE methods. *Journal of Computational Physics*, 229(20):7649 – 7671, 2010.
44. T. Sorokina and A.J. Worsey. A multivariate Powell–Sabin interpolant. *Advances in Computational Mathematics*, 29(1):71–89, 2008.